Environmental Science and Pollution Research (2022) 29:4311–4333
https://doi.org/10.1007/s11356-021-15554-2

RESEARCH ARTICLE

Integrated approach for the evaluation of groundwater quality through hydro geochemistry and human health risk from Shivganga river basin, Pune, Maharashtra, India

Ajaykumar Kadam[1] · Vasant Wagh[2] · James Jacobs[3] · Sanjay Patil[4] · Namdev Pawar[5] · Bhavana Umrikar[6] · Rabindranath Sankhua[7] · Suyash Kumar[8]

Received: 19 January 2021 / Accepted: 17 July 2021 / Published online: 17 August 2021

Abstract

The present study is focused on seasonal variation in groundwater quality, hydrochemistry, and associated human health risk in the Shivganga river basin, Western Maharashtra, India, to promote sustainable development of groundwater resources of this semi-arid region. The qualitative geochemical analysis, contamination levels, and human health risk assessment (HHRA) of groundwater are integral steps in groundwater management in the Deccan Plateau basalt flow region of India. Representative groundwater samples ($n = 68$) collected from the Shivganga River basin area of Pune district, Maharashtra, during pre-monsoon (PRM) and post-monsoon (POM) seasons in 2015 were analyzed for major cations and anions. According to the World Health Organization (WHO, 2017) drinking standards, EC, total dissolved solids, hardness, bicarbonate, calcium, and magnesium surpassed the desirable limit. Boron and fluoride content exceeded the prescribed desirable limit of the WHO. The pollution and drinking suitability were assessed by computing pollution index of groundwater (PIG), groundwater quality index (GWQI), and HHRA particularly for boron and fluoride toxicity. PIG values inferred that about 6% of groundwater samples has moderate, 24% has low, and 70% has insignificant pollution in the PRM season, while only 1 sample (3%) showed high pollution, 6% showed low, and 91% showed insignificant pollution in the POM season. GWQI classification demonstrated that 27% and 15% samples are within the poor category, and only 15% and 18% of the samples fall into excellent water category in the PRM and the POM seasons, respectively. Total hazard index (THI) revealed that 88% of children, 59% of adults, and about 38% of infants are exposed to non-carcinogenic risk, as THI values (>1) were noted for the PRM season, while 62% of children, 47% of adults, and 24% of infants are vulnerable to non-carcinogenic health hazard during the POM period.

Responsible editor: Xianliang Yi.

✉ Vasant Wagh
wagh.vasant@gmail.com

Ajaykumar Kadam
kadamajaykumar1@gmail.com

James Jacobs
geojimj@gmail.com

Sanjay Patil
drsnpatil9@gmail.com

Namdev Pawar
dr.njpawar@gmail.com

Bhavana Umrikar
bnumrikar@gmail.com

Rabindranath Sankhua
sankhua12@yahoo.com

Suyash Kumar
suyashgwl@gmail.com

[1] Department of Environmental Sciences, Savitribai Phule Pune University, Pune, Maharashtra, India

[2] School of Earth Sciences, Swami Ramanand Teerth Marathwada University, Nanded, Maharashtra, India

[3] Clearwater Group, 229 Tewksbury Avenue, Pt. Richmond, CA 94801, USA

[4] Department of Applied Geology School of Environmental & Earth Sciences, KBC North Maharashtra University, Jalgaon, Maharashtra 425 001, India

[5] Dr. D. Y. Patil Vidyapeeth, Pune, India

[6] Department of Geology, Savitribai Phule Pune University, Pune 411007, India

[7] Basin Planning, Central Water Commission, New Delhi 110066, India

[8] Department of Geology, Govt. P G Science College, Gwalior 474009, India

Keywords Shivganga river · Groundwater quality index · Pollution index of groundwater · Human health risk assessment · Drinking suitability

Introduction

Groundwater is the primary source of freshwater for drinking, irrigation, and industrial uses in most of the developing countries. As concern to India, during the last five decades, growth in population and economic expansion, the groundwater-based agriculture sector contributed nearly 46% of the gross national product and played an important role in financial growth of the country (CGWB 2010). Due to rapid growth in agriculture, groundwater in many parts of the country is under severe stress and resulted in the depletion of groundwater quality as well as a decline in groundwater quantity particularly in hard rock terrains (Pawar et al. 2008; Sonkamble et al. 2012; Thomas et al. 2015; Sethy et al. 2016). Over the past few years, in India, people have progressively experienced the groundwater pollution problems and its revitalization; therefore, many theoretical and applied studies have been executed in different regions to evaluate groundwater quality for drinking, industry, agriculture, etc. Many water researchers studied the source of groundwater contamination through hydrochemical, hydrogeochemical, and health risk assessment methods, and which confirmed to be a helpful tool for distinguishing groundwater composition and quality in a more scientific approach (Subba Rao et al. 2019, 2020; Haji et al. 2021). Therefore, sustainable use of groundwater resources and its protection are of vital importance to public health and the economy of India and in particular, this region of the state of Maharashtra. Generally, the chemical concentration in groundwater is influenced by natural factors including water-rock contacts, groundwater residence time, and ion exchange processes. Anthropogenic factors included agricultural practices using chemicals and fertilizers, industrial waste processes, mining activities, etc., altered groundwater composition (Adimalla et al. 2018; Gaikwad et al. 2020a). Subba Rao et al. (2019) investigated the controlling factors of groundwater composition through Gibbs plot, Piper diagram, bivariate diagrams, etc. which helps to recognize soil–rock–water connections, dissolution and weathering, ion exchange and evaporation processes are dominant in altering groundwater chemistry in various parts of Andhra Pradesh, India.

In recent years, some of the pollutants like fluoride, boron, and nitrate have widely impacted groundwater and cause carcinogenic and non-carcinogenic impacts on human health (Subba Rao et al. 2017; Adimalla 2019a, b; kadam et al. 2019; Wagh et al. 2020a). Human health-related risk assessment (HERA) was developed by the United States Environmental Protection Agency (USEPA 1980). It is used to evaluate the nature and potential undesirable effects on health of people due to drinking contaminated water (Li et al. 2016; Zhang et al. 2018; Kawo and Karuppannan 2018). As concerned with Maharashtra state, districts like Chandrapur, Gadchiorli, Nagpur, and Nanded are prone to fluoride problems. The possible sources of fluoride in these regions are leaching fluoride containing minerals from granitic exposures in a semi-arid condition with alkaline waters (Kadam et al. 2019; Pandith et al. 2017; Panaskar et al. 2017). Thus, it is a crucial and challenging task for water researchers to detect the origin and occurrence of fluoride and their possible health impacts for efficient groundwater resource management.

Groundwater pollution in hard and fractured rock topographies like the Deccan Plateau basalt provinces is a continuous but variable process due to lithologic heterogeneity and comparatively uneven flow of rainwater in fractured and weathered basalt aquifers. There is also the preponderance of lesser amount of subsurface groundwater movement resulting in a high rock-water reaction time. Moreover, in some isolated areas where large fractures within the basalts do not intersect, the groundwater travels slowly through the aquifer media, unconnected in the phreatic zone to other more regional aquifers. In several studies, under natural condition, this mechanism is favorable for raising the pollutant content due to prolonged rock-water interactions. Furthermore, the geochemistry of groundwater in phreatic aquifers of the hard rock volcanic provinces is potentially vulnerable by anthropogenic inputs such as unrestricted industrialization; metropolitan landfill use, and stormwater flow from the agricultural sector (Balamurugan et al. 2020; Mukate et al. 2020; Kale et al. 2010). A couple of investigations have been carried out on hydro-geochemical classification and groundwater contamination caused by anthropogenic activities (Wagh et al. 2017; Adimalla et al. 2020). The hydro-geochemical studies become crucial to distinguish the discrepancies in ionic concentrations for utilization in various sectors; therefore, various hydro-geochemical methods were exercised to evaluate groundwater composition in the respective regions (Ledesma-ruiz et al. 2016; Panneerselvam et al. 2020). Consequently, several new studies have been introduced for the interpretation of the cations, anions, and heavy/trace metals in the groundwater, to distinct the natural and anthropogenic origins that alter groundwater quality and their associations within the aquifer system (Tian et al. 2015; Brindha et al. 2017; Wagh et al. 2018). The previous works carried out in the Deccan Volcanic Provinces-Western Ghat (DVP-WG) have mainly focused on the hydro-geochemical evolution in the groundwater (Pawar et al. 2008; Vincy et al. 2015; Wagh et al. 2019a, b). However, several studies were addressed the crisis of groundwater pollution due to agriculture activities, industrialization, and urban growth in DVP-WG region (Pawar and Shaikh 1995; Wagh et al. 2016a, b).

The Shivganaga region belongs to DVP-WG region of Maharashtra, India. Limited research work on groundwater contamination, quality, and associated health risk to inhabitants is relatively sparse until recently (Kadam et al. 2021a, b). The governing factors on fluoride and boron enrichment and health risk are not consistent, even similar climatic and hydrogeological conditions. Usually, in the alluvium plain, the shallow aquifers are more susceptible to alteration than the deeper basaltic aquifers because of high transmissivity and porosity of the soil and rocks. In the studied region, dug wells commonly provide water for domestic and irrigation needs; therefore, the groundwater quality is intimately linked with local inhabitants. Therefore, frequent monitoring and suitability appraisal of groundwater quality is an essential to avoid further human health deterioration in portions of the study area having elevated pollution levels. Hydro-geochemical studies are required to recognize the mechanism of natural and anthropogenic processes concerned with alteration of groundwater quality. Infiltrated recharged water interacts with soil including physical, chemical, biological processes, and mineral dissolution takes place, impacting the chemical constituents of the groundwater. In general, in this study, hydrogeochemical processes which are mainly accountable for changing the chemical composition of groundwater varied with respect to time and space. Therefore, the study was carried out with the main objectives (1) to assess the seasonal variation in hydro-geochemistry of groundwater and identify the influencing parameters altering groundwater quality, (2) to assess the groundwater contamination and degree of pollution level through GWQI and PIG methods and prepare a spatial interpolation maps to understand the seasonal variation in groundwater quality, and (3) to evaluate human health risk from groundwater suitability perspective and recognize the processes which control groundwater composition in the study area. In sum, outcomes of the study will provide scientific data on source and history of groundwater contaminants in the studied region. Also, the objective is to help governing bodies, water planners, and resource managers to develop effective basin management plans in semi-arid western parts of the DVP.

Geo-environmental outline

The Shivganga River basin (latitudes 18°13′36″ and 18°24′7; longitudes 73°44′1″and 73°56′17″) flows within a small basin of about 176 km^2, situated on the easterly sloping face of the Western Ghat region, Maharashtra state, India. The area is drained by a fifth order, 27-km-long Shivganga River (Fig. 1). The study area is encompassing undulating topography with elevated hill ranges originating from Deccan Trap basaltic flows; the highest peak being 1316 m above mean sea level (amsl) and lowest at mouth of the river 590 m amsl. The area represents a tropical monsoon climate and obtains yearly rainfall of ~900 mm from the southwest monsoon in the month of

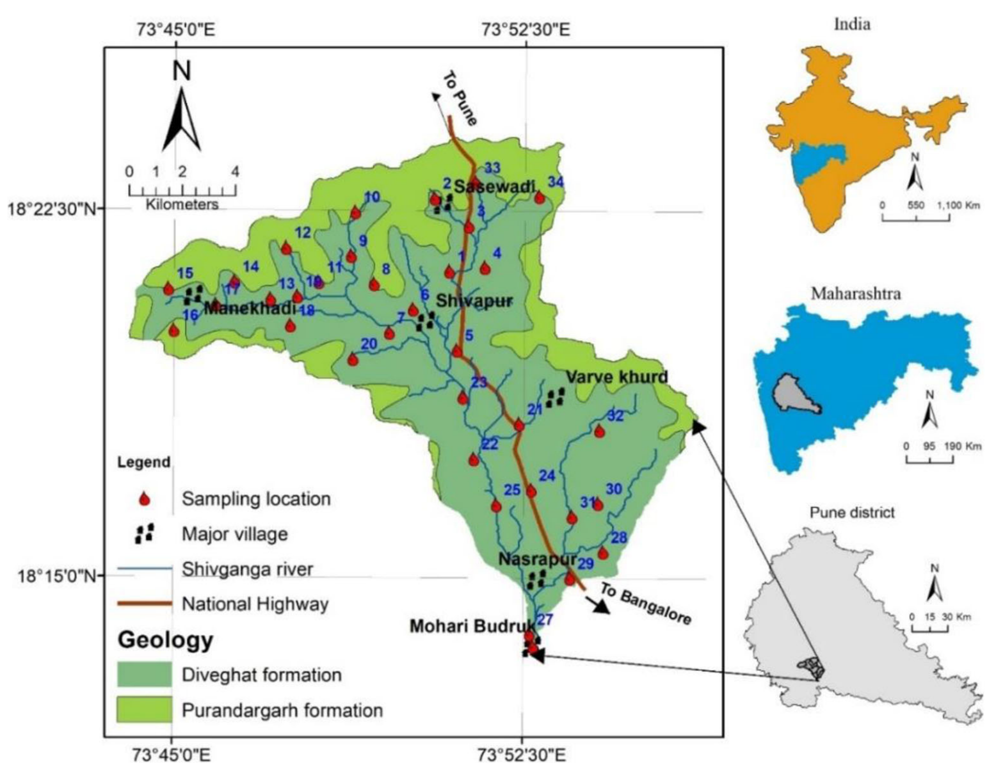

Fig. 1 Shivganga watershed with groundwater sample stations

June and September. Also, a wide range of temperature variation occurs in winter (10°C) and summer (39°C). The two main cropping seasons with irrigation-based agriculture Kharif (July–October) and Rabi (October–January) are assigned to rice paddies and jowar (sorghum) fields for the major crop cultivation in the area. The study area shows mainly five land use and land cover classes: irrigated crop land (45.14%), residential and paved land (6.38%), surface water reservoir (0.57%), forest and plantation land (27.75%), and barren land (19.16%) (Kadam et al. 2018). Forest cover is observed at high elevation, in the peripheral areas representing river catchment. Due to major consumption of groundwater for agricultural and domestic needs, groundwater levels are going down very quickly in the area and are not rebounding. Also, the study area is restraining growth of 58 large villages having around 0.07 million population (Census of India 2011). This lack of available water resources exerts pressure on excess groundwater pumping, resulting in overexploitation and contamination of groundwater in study area (Kadam et al. 2018). The study region consists of little primary porosity in the form of basalt vesicles (air bubbles) which do not support transmission of groundwater as they are not interconnected. Hence, the groundwater potential in this area is primarily governed by permeability and increased of secondary porosity by compressional, tensional forces and rapid cooling of magma leading to weathering and fracturing in the basaltic terrain. In the area, the depth of weathered rocks are 1–16m and fractured rocks 12–60m below ground level (bgl) (CGWB 2013). The weathered zone comprises black cotton alluvium soil derived from basalts and clayey soil derived from red interflow horizon, which is a break between two successive lava flows. As clay is characterized by micro porosity, the infiltration capacity of water is negligible, which in turn retards groundwater movement. So, in the weathered zone, groundwater occurs in water table phase and fractured/jointed aquifers under semi-confined conditions. The water table depth varies from less than 4m to more than 12m bgl, based on the varied topographic features.

As per the cross section of the hydrogeological conditions drawn in the upstream part to downstream part side based on the dug well section, bore well drilling and previous unpublished work as well as geophysical survey work are presented for this study area (Fig. 2); the depth of surface soil changes from 1 to 5m from the ground surface from the peripheral part of sample number 12 to the mouth of the river at sample number 27. Subsequently, the depth of highly to moderately weathering host rock, which primarily decreases the permeability, the weathering thickness of the rock ranges from 1 to 24m. This condition is categorized by low porousness owing to isolated minute voids in the weathering basalt rock. The lack of connected porosity restricts liquid movements inside these rock layers. The next layer down is the fractured basalt having depth ranges between 10 and 35 m, which is characterized by high porousness, since these are continuously connected to the pore spaces in the rock-fractured zone that allow the groundwater movement to flow easily from one point to next point. The lithology in this zone shows vesicles in the form of primary porosity which acts as a storage for the groundwater. As these vesicles are not interconnected, the flow and movement of groundwater is partially restricted. The compact massive basalt occurred beneath the vesicular basalts and lacks in the capability of water storage and blocks the movement of groundwater. The above lithologic characteristics are generally observed in the aquifers in the study area.

Material and methods

In the survey of India (SOI), topographic sheets (numbers 47F/15 and 47F/16) on 1.50,000 scales have been used for preparation of a base map of the study area including major features such as the road network, streams, and settlements. In the study area, a groundwater comprehensive assessment was performed using a collection of sixty-eight dug well water samples in the year of 2015 during pre-monsoon and post-monsoon seasons (May and November) with respect to land use, lithology, landform, and use in drinking based on random sampling method. The groundwater has been sampled in pre-washed 0.5-l polytene bottles and kept in temperature below 4°C in the laboratory to avoid further reaction. The

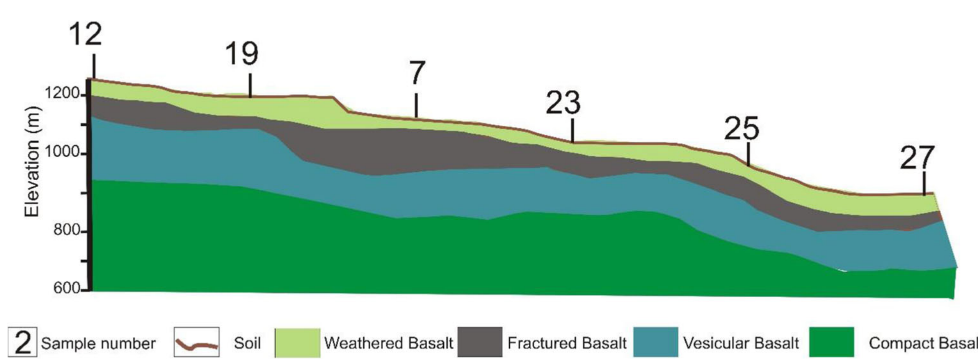

Fig. 2 Cross-section profile showing the major litho units in the study area

coordinates of each sampling location were collected by GARMIN GPS for preparation of base map as well as for identification and validation of land use land cover study. Also, these location coordinates were used for the preparation of spatial interpolation maps. The potential of hydrogen ion (pH), electrical conductivity (EC), and total dissolved solid (TDS) was measured on-site using calibrated digital handheld pH, EC, and TDS meters. The separate 100 ml samples were also collected in acidified bottles with 0.5 ml nitric acid for reduced precipitation of major salt. The major ions such as calcium (Ca^{2+}), magnesium (Mg^{2+}), bicarbonates (HCO_3^-), and chlorides (Cl^-) were analyzed by standard titrimetric methods. Sodium (Na^+) and potassium (K^+) ions were estimated by flame photometric method (ELICO CL 3610). Boron (B^{3+}) and fluoride (F^-) were analyzed by HPIC (Dionex make DX-600). Also, nitrate (NO_3^-) and sulphate (SO_4^-) were measured by a spectrophotometer (Shimadzu UV-800) as per the standard procedures of water and wastewater analysis (APHA 2005). The charge balance errors (CBE) were observed within the allowable limit of ± 10% (Berner and Berner 1987). The analyzed results were presented on piper tri-linear diagrams using Aqua-chem 4.0 software to understand the dominant hydro-geochemical facies and Gibbs diagrams were prepared to evaluate the quality regulatory mechanism. The analyzed sample results were compared to the World Health Organization (WHO, 2017) drinking standards for drinking and household purposes. The analyzed samples were also used in the computation of the groundwater quality index (GWQI) and pollution index of groundwater (PIG). To understand the health impact on inhabitants, the human health risk assessment (HHRA) is calculated for oral and dermal exposure pathways for B and F by following USEPA guidelines. MS Excel was used for statistical analysis.

Computation of groundwater quality index

Computation of groundwater quality index (GWQI) is widely used technique to categorize the groundwater quality as: excellent, good, poor, very poor, and unsuitable for drinking. It is based on the rank and weights given to the analyses parameter and it is one of the most trusted indices for the quality assessment of groundwater. For the comprehensive assessment of groundwater quality and suitability, the water quality parameters such as pH, TDS, Ca^{++}, Mg^{++}, TH, Na^+, K^+, HCO_3^-, Cl^-, SO_4^-, PO_4^-, NO_3^-, B^{3+}, and F^- were considered. The GWQI calculated by the following steps.

Step 1. Allotted the weight (AW) to each analyzed parameter considering its importance to overall body growth (Table 1);

Step 2. Computation of relative weight (RW) for each water quality parameter (Eq. (1)).

$$\mathrm{Rw} = \mathrm{Aw}/\sum\nolimits^{n}{}_{\mathrm{i}} W \tag{1}$$

where W is the sum of all allotted weight; and n is the number of groundwater quality parameter

Step 3. Computation of quality rating scale (QRS) of each groundwater quality parameter (Eq. (2))

$$\mathrm{QRS} = (\mathrm{CP}/\mathrm{SWHO}) \times 100 \tag{2}$$

where the CP stands for the content of each parameter in groundwater and SWHO stands for standard limit of the WHO of the respective parameters.

Step 4. The calculation of the GWQI, which the summation of sub-index (Sbi),

Where, Sbi is the multiplication of relative weight (RW) by quality rating scale (QRS) of each groundwater quality parameters (Eqs. (3) and (4)), (Table 1).

$$\mathrm{Sbi} = \mathrm{RW} \times \mathrm{QRS} \tag{3}$$

$$\mathrm{GWQI} = \sum \mathrm{Sbi} \tag{4}$$

Computation of pollution index of groundwater

Pollution index of groundwater (PIG) is a numerical expression for rating the quantifying range of contamination by considering parameters such as pH, TDS, major cations and anions, boron, and fluoride based on their relative importance in defining groundwater quality (Rao and Chaudhary 2019; Wagh et al. 2020b). PIG was based on considering WHO drinking standards, also computed by following the methodology proposed by Subba Rao (2012).

To generate the index values, firstly, a relative weight (Rw) was assigned to each of the water variables. The Rw values ranges between 1 and 5; where, 1 is having the least importance in health risk due to low pollution, while 5 having the highest importance for health risk due to high pollution. Potassium has an assigned Rw value of 1 and calcium and magnesium have an assigned Rw value of 2. Bicarbonate has an assigned Rw value of 3. Chloride has an assigned Rw value of 4, and the assigned maximum values of 5 are for pH, TDS, boron, and fluoride (Table 2).

The weight parameter (Wp) is calculated by the ratio of relative weight (Rw) of each parameter to the sum of all Rw values, presented by following Eq. (5):

Table 1 Allotted weights and relative weights of physiochemical parameters

Chemical parameters	WHO standards (2017)	Allotted weight (Aw)	Relative weight (Rw)
pH	8.5	4	0.075
EC	500	4	0.075
TDS	500	5	0.094
TH	100	3	0.057
Ca^{2+}	75	3	0.057
Mg^{2+}	50	3	0.057
Na^{+}	200	2	0.038
K^{+}	10	2	0.038
Cl^{-}	250	5	0.094
HCO_3^{-}	500	1	0.019
SO_4^{-}	250	5	0.094
NO_3^{-}	45	5	0.094
PO_4^{-}	0.5	1	0.019
F^{-}	1.0	5	0.094
B^{3+}	1.0	5	0.094
		53	1.000

$$\mathrm{Wp} = \mathrm{Rw}/\sum \mathrm{Rw} \tag{5}$$

Further, statues of concentration (Sc) are calculated with Eq. (6):

$$\mathrm{Sc} = (C/\mathrm{Ds}) \tag{6}$$

where C is the concentration in each groundwater samples; Ds is drinking water quality standard.

The overall water (Ow) quality is multiplication function of weight parameter (Wp) with statues of concentration (Eq. (7)):

$$\mathrm{Ow} = \mathrm{Wp} \times \mathrm{Sc} \tag{7}$$

Finally, PIG is calculated by summation of overall water quality (Ow) computed by Eq. (8):

$$\mathrm{PIG} = \sum \mathrm{Ow} \tag{8}$$

Computation of human health risk assessment

Human health risk assessment (HHRA) is computed based on daily intake, dermal contact, and inhalation (He et al. 2020). Moreover, consumption of water with elevated boron and fluoride concentrations may result a non-carcinogenic risk to inhabitants. Thus, three age groups were considered: infants 6 months (0.5 years); children up to age 6 year and adults (≥16 years) (Kadam et al. 2019).

The value of estimated daily intake (EDI) of the above age groups for F and B content in groundwater was computed by Eq. (9) (USEPA 1989; Zango et al. 2019).

$$\mathrm{EDI} = \left\{C_{(\mathrm{F,B})} \times \mathrm{Cd}\right\}/\mathrm{Bw} \tag{9}$$

where EDI having unit mg/kg/day; C (F, B) is content of F or B in groundwater; Cd indicates every day average ingestion of water and Bw denotes body weight. Cd value for adults is 3L/day, children 1.5 L/day, and infants 0.250 L/day (Vetrimurugan et al. 2013). However, Bw for adults is 57.5 kg, children 18.7 kg, and infants 6.9 kg ICMR Expert Group (1990)

Table 2 Details of PIG (after Wagh et al. 2020b)

Parameter	Relative weight (Rw)	Weight Parameter (Wp)	Drinking water quality standard Ds*
pH	5	0.109	8.5
TDS	5	0.109	500
Ca^{++}	2	0.043	75
Mg^{++}	2	0.043	30
Na^{+}	4	0.087	200
K^{+}	1	0.022	10
HCO_3^{-}	3	0.065	300
Cl^{-}	4	0.087	250
SO_4^{-}	5	0.109	150
NO_3^{-}	5	0.109	45
F^{-}	5	0.109	1
B^{3+}	5	0.109	1
Sum (∑)	46		

*All values in mg/L expect pH

The hazard quotient (HQ) was determined for groundwater by F and B exposure to individuals was projected from Eq. (10) (USEPA 1989), and it is the ratio of EDI to the reference dose (Rfd)

$$HQ = EDI/Rfd \tag{10}$$

where the RfD value of F (0.06 mg/kg/day) was considered from the US Environmental Protection Agency (USEPA 2014) guideline, while the RfD of B (0.13 mg/kg/day) was obtained from WHO (2009).

Finally, total hazard index (THI) was calculated for the human health risk of F and B; it is the summation of hazard quotient of fluoride plus hazard quotient of B.

Results and discussion

Seasonal variation in hydro-geochemistry

The statistical summary of physicochemical parameters for the pre-monsoon (PRM) and post-monsoon (POM) seasons of year 2015 and its comparison with the WHO drinking standards (2017) are illustrated (Tables 3 and 4). The measured pH value in PRM season ranges from 7.44 to 8.38 due to the bicarbonate form of liquified carbonate in water. However, during POM season, it varies from 6.85 to 7.51 showing the natural range due to rainwater dilution of rainwater alkalinity. Accordingly, groundwater shows moderately alkaline nature in both seasons of the study area. The groundwater samples of both seasons are within the threshold limit (6.5–8.5) of the WHO (2017) drinking norms (Table 4). Groundwater had a slight decrease in pH from PRM to POM season which indicates a good rock-water interface. The electrical conductivity (EC) values are within the ranges of 296 to 1070 μS/cm (avg. 635μS/cm) and 240 to 980 μS/cm (avg. 589μS/cm) in the PRM and POM groundwater samples respectively (Table 3). EC was increased during the PRM season which may be due to the evaporation of soil moisture from the phreatic zone as well as prolonged rock-water reaction and manmade contamination by concentration, causing increases in ionic content (Wagh et al. 2020b). According to WHO standards, 80 and 68% samples are higher than the recommended range of 500μS/cm for both the seasons (Table 4).

TDS values representing total positive and negative ionic contents in water vary from 196 to 832 mg/L (avg. 404 mg/L) and 164 to 591 mg/L (avg. 383 mg/L) in PRM and POM seasons, respectively (Table 3). As compared to WHO standards, desirable limit (DL) is 500 mg/L of TDS, and 24% in PRM and 15% in POM samples are above the DL (Table 4). Also, the high content of TDS is possibly related to root exudation of aquifer media salts from the surface soil and certain manmade actions (Mukate et al. 2019). However, during the POM season, the concentration of these parameters has decreased due to dilution by fresh rainwater recharge in the aquifer system. High contents of EC and TDS were detected in the groundwater samples in the lower reach of the study area owing to accumulation of salt from agricultural activities. Total hardness (TH) content ranges from 52 to 604 mg/L with (avg. 234 mg/L), and as per WHO standards, 95% samples above DL of (500 mg/L) in the PRM season. TH content for the POM season varied from 96 to 384 mg/L with average value of (248 mg/L); 97% samples were detected above the DL (Table 4). The standard deviation values of TH were also very high in both seasons representing the local effect on the groundwater quality which reflected in the minimum and maximum values of groundwater samples. Sample number 5 had a TH content over the PL threshold (>500 mg/L), due to the salt deposition on the inner lining on the well due the long rock-water interaction.

TH values obtained in groundwater were divided in four classes following Sawyer and McCarty (1967) classification.

Table 3 Statistical summary of groundwater analysis from pre-monsoon and post-monsoon seasons

	pH	EC	TDS	TH	Ca^{2+}	Mg^{2+}	Na^{+}	K^{+}	PA	HCO_3^-	Cl^-	SO_4^-	NO_3^-	PO_4^-	B^{3+}	F^-
PRM 2015																
Max.	8.38	1070	832	604	120	74	109	7.78	100	320	248.5	151.24	18.65	0.32	12.45	1.84
Min.	7.44	296	196	52	8	8	10	0.2	0	30	19.1	12.32	6.39	0.02	0.08	0.1
Average	7.74	635.3	404	234	52	26	27	1	27	168	77.59	42.17	12.52	0.05	3.97	0.84
Std. dev	0.21	186	141	103	25	13	16	1.78	31	67	42.2	32.31	2.7	0.05	3.51	0.4
POM 2015																
Max.	7.51	980	591	384	90	55	24	3.2	60	360	62.12	85.2	13.95	2.9	14.33	1.48
Min.	6.85	240	164	96	13	3	5	0.02	0	100	3.85	10.2	0.12	0	0.34	0.02
Average	7.22	589	383	248	56	23	14	0.38	28	240	17.01	32.74	3.43	0.11	3.15	0.63
Std. dev	0.14	170	102	81	15	11	5	0.61	12	62	13.87	19.76	3.46	0.49	3.45	0.37

All values denoted in mg/L; except pH on scale; EC in uS/cm

Table 4 Physicochemical parameters of groundwater and its comparison with WHO drinking standards (WHO 2017)

Parameters	WHO standards* 2017 DL-PL	PRM 2015		POM 2015	
		% samples above DL	% samples above PL	% samples above DL	% samples above PL
pH	6.5–8.5	–	–	–	–
EC	500–1500	80	–	68	–
TDS	500–1500	24	–	15	–
TH	100–500	95	3	97	–
Ca^{2+}	75–200	18	–	6	–
Mg^{2+}	50–100	3	–	3	–
Na^{+}	200–600	–	–	–	–
K^{+}	10–12	–	–	–	–
HCO_3^-	200–500	30	–	76	–
Cl^-	250–500	–	–	–	–
SO_4^-	200–250	–	–	–	–
NO_3^-	45	–	–	–	–
F^-	1–1.5	35	6	18	–
B^{3+}	0.5–1.0	70	58	51	39

* All values in mg/L, except pH and EC in uS/cm

DL desirable limit, *PL* permissible limit

The soft water sample having TH values less than 75 mg/L (sample number 26) is found in this class the PRM season; whereas, no samples were in this class from the POM season. The moderately hard water having TH concentration ranges from 75 to 150 mg/L having classification present shows that only eight samples (sample numbers 7, 9, 11–14, 16, 27), i.e., 21% belongs to moderately high TH class in the PRM season, while only 4 samples (sample numbers 23–26) (i.e., 12%) were in the moderately high TH class in the POM season. The hard water classification has a TH value range from 150 to 300 mg/L and 49% and 53% samples were in this category in both the PRM and the POM seasons. Also, 24% and 35% samples show very hard range in both the seasons. A meager rise has been observed in water hardness during POM season but the majority of the samples fall in the hard and very hard categories.

In the study area, the POM samples represent the cation dominance in decreasing order of Ca^{2+}> Mg^{2+}> Na^+> K^+ due to dissolution of aquifer minerals with rainwater. Whereas, Ca^{2+}> Na^+> Mg^{2+}> K^+ in the PRM seasons are the result of evaporation dominance, anthropogenic inputs, and irrigation practices. The Ca^{2+} contents are found within the range of 8 to 120 mg/L averaging of 50 mg/L and 13 to 90 mg/L (avg. 46 mg/L) in both PRM and POM periods, respectively (Table 3). The calcium content varies with the monsoon; if rainfall decreases in the pre-monsoon season, the calcium concentration increased significantly. Thus, ~18% samples of the PRM season and only 6% samples in the POM period are beyond the DL (75 mg/L) of the WHO (Table 4). Moreover, Mg^{2+} occurred in ranges of 8 to 74 mg/L (avg. 26 mg/L) and 3 to 55 mg/L (avg. 23 mg/L) in the PRM and the POM seasons, respectively (Table 3). High content of Mg^{2+} is most probably due to the higher rate of irrigation return flow, which increases the dissolution of evaporite minerals and subsequently increase concentration of magnesium in groundwater within the shallow aquifers especially in low-lying regions of the watershed (Haritash et al. 2008). As per WHO drinking standards, all the samples are suitable for drinking; however, only 3% samples surpass the DL in the PRM and the POM seasons respectively (Table 4). Also, diminutive content of Na found with an average value of 27 mg/L and 14 mg/L in the PRM and the POM seasons (Table 3). As compared to other common cationic constituents occurring in water, the potassium concentration is low due to the high resistance of this element in the clay mineral structure (Srinivas et al. 2017). Generally, potassium content in natural hydrological cycle varies from 0.1 ppm in rainwater to a few ppm in surface water and groundwater (Matthess 1982). In the area, average K^+ values are 0.93 mg/L and 0.99 mg/L in the pre-monsoon and the post monsoon seasons (Table 3). It is observed that all the samples having content of sodium and potassium are within threshold limit of the WHO.

The anion abundance was observed in order of HCO_3– > Cl–> SO_4^{2}–> NO_3–> PO_4^{2-} in the pre-monsoon season, while in the post-monsoon season HCO_3–> SO_4^{2}–> Cl– > NO_3– > PO_4^{2}–. It is observed that HCO_3– content varies from 30 to 320 mg/L with an average value of (168 mg/L) and 100 to 360 mg/L (avg. 240 mg/L) in the PRM and the POM seasons

(Table 3). Moreover, it is inferred that due to alkaline condition of water, carbonate species be present in the form of bicarbonate. Results indicated that 30% and 76% of groundwater samples exceeded the permissible limit of the WHO in the PRM and the POM seasons, respectively (Table 4). The elevated content of HCO_3^- in few groundwater samples is due to agricultural runoff as well as from basaltic host rock (Locsey and Cox 2003). SO_4^{2}– content varies with ranges of 12 to 151 mg/L with an average value of (4.17 mg/L) and 10 to 85 mg/L (avg. 32.74) in the PRM and the POM seasons, respectively. The excessive concentration of SO_4^{2}– in the POM season is due to the addition of manmade as activities involving detergents and fertilizers. Chloride content varies from 19 to 249 mg/L and 4 to 62 mg/L with an average values of (78 mg/L and 17 mg/L) in the PRM and the POM seasons, respectively. It is pragmatic that high content of chloride is present in the PRM season; however, low chloride content in the POM season is due to dissolution phenomenon. High chloride content is attributed to secondary sources like domestic sewage including human fecal material, decomposition of carbon-based substances, and agrarian surface flow (Mukate et al. 2017; Kumar et al. 2008). NO_3– content ranges from 6 to 19 mg/L (avg. 13 mg/L) and 0.12 to 14 mg/L (avg. 3 mg/L) during the PRM and the POM seasons, respectively (Table 3). According to WHO specifications, all groundwater samples are suitable for drinking. PO_4^{2}– values vary within ranges of 0.02 to 0.32 mg/L (avg. 0.05 mg/L) in the PRM season and below detection limit to 2.90 mg/L (avg. 0.11 mg/L) in the POM season (Table 4). However, high content in the POM season is due to agricultural return flow from the irrigation fields (Vetrimurugan et al. 2013).

Boron content varies from 0.08 to 12.45 mg/L (avg. 3.97 mg/L) during the PRM season; conversely, 0.34 to 14.33 mg/L with (avg. 3.15 mg/L) in the POM season (Table 3). As compared with WHO standards (Table 4), 70% and 51% of samples exceed the DL (0.5 mg/L) for the PRM and the POM seasons, respectively, while 58% and 39% of the samples are above the PL (1 mg/L) in the PRM and the POM seasons, respectively. The spatial variation maps (Fig. 5a, b) demonstrate that the PRM season samples have higher concentrations of boron as compared to the POM season samples. The possible source of boron in groundwater is from the rock-water interaction, sewage effluent, and fertilizer application (Bhat et al. 2018). The high concentration of boron in study area is due to agricultural runoff, excessive use of herbicides and manures, and inputs from poultry farming and animal excreta (kadam et al. 2019). The surplus content of boron is toxic to human health and crops; it also reduces the soil productivity (Ahmad et al. 2012; USEPA 2008).

Generally, fluoride is one of the primary trace element in sub-surface water, which is essential for human health; but, when it exceeds the allowable content, fluoride poses serious human health hazards (Kale and Pawar 2017; Das and Nag 2017; Panaskar et al. 2017). The host rock with F bearing minerals acts as a source and is accountable for the elevated F content groundwater (Kale et al. 2010). F content varies from 0.10 to 1.84 mg/L with an average value of (0.84 mg/L) during the PRM season, while 0.02 to 1.48 mg/L (avg. 0.63 mg/L) in the POM season (Table 3). As per the WHO drinking specifications (Table 4), fluoride content in the PRM (35%) and the POM (18%) seasons showed groundwater samples above the DL (1 mg/L). However, only (6%) of the groundwater samples exceed the PL (1.5 mg/L) in the PRM season; thus, elevated F restricts drinking water use in two locations (numbers 13 and 28). However, those sampling locations are beyond the PL (1.5 mg/L) for F and may lead to dental fluorosis and skeletal deformities in the study area; so, groundwater in those locations is unfit for human consumption. The elevated content of F in the PRM season is due to semi-arid condition with evaporation; alkaline water in the study area is more favorable for dissolution of fluorite mineral (Chen et al. 2017; Kadam et al. 2019). Also, fluoride-rich minerals like fluorite, muscovite, biotite, topaz, apatite, and hornblende, from host rocks in the area, are the possible sources of leaching of F ion into the groundwater (Rao et al. 2020; Narsimha and Li 2019).

$$\begin{aligned} &K\,(Mg, Fe)\,AlSi_3O_{10}\,(OH, F)_2 + 5H_2O \\ &\quad + 4CO_2 \qquad K + Mg + Fe\,(OH)_3 + 4HCO_3 + H \\ &\quad + 2F + Al_2Si_2O_5\,(OH)_4 + 2SiO_2\ (\text{Biotite}) \end{aligned} \tag{11}$$

$$\begin{aligned} &Ca\,Na\,(Mg, Fe, Al)\,(Si_7Al)\,O_{22}\,(OH, F)_2 + H_2O \\ &\quad + CO_2 \qquad Ca + Mg + Na + Fe\,(OH)_3 + HCO_3 \\ &\quad + 2F + Al_2Si_2O_5(OH)_4 + SiO_2\ (\text{Hornblende}) \end{aligned} \tag{12}$$

Based on Eq. (11), when groundwater charged with CO_2 reacts with biotite minerals, the ions such as K, Mg, HCO_3, F, and SiO_2 enter into the groundwater from aquifer matrix. Thus, the high bicarbonate leached from aquifer matrix in groundwater facilitates release of large concentrations of fluoride ions from the host rock into groundwater. The scatter plot of Mg+K vs HCO_3+F (Fig. 3) shows noteworthy positive correlation (r= 0.54) confirming the process in Eq. (11). Based on Eq. (12), the reaction suggested that rock mineral deposits of hornblende with subsurface water (H_2O) and atmospheric CO_2 react with ions such as calcium, magnesium, sodium, and bicarbonate. F and SiO_2 are released into groundwater from the host rock. The scatter plot of Ca+Mg+Na vs HCO_3+F (Fig. 4) shows strong positive correlation (r= 0.72) which suggests that the weathering of hornblende mineral is related to the increased content of ions including fluoride ions in groundwater. Both Eqs. (11) and (12) show that Deccan Plateau rain water is highly alkaline, having a pH above 7.5. Generally, rainwater leaches surface minerals and enters the

Fig. 3 Correlation between the concentration of Mg+K vs HCO_3+F

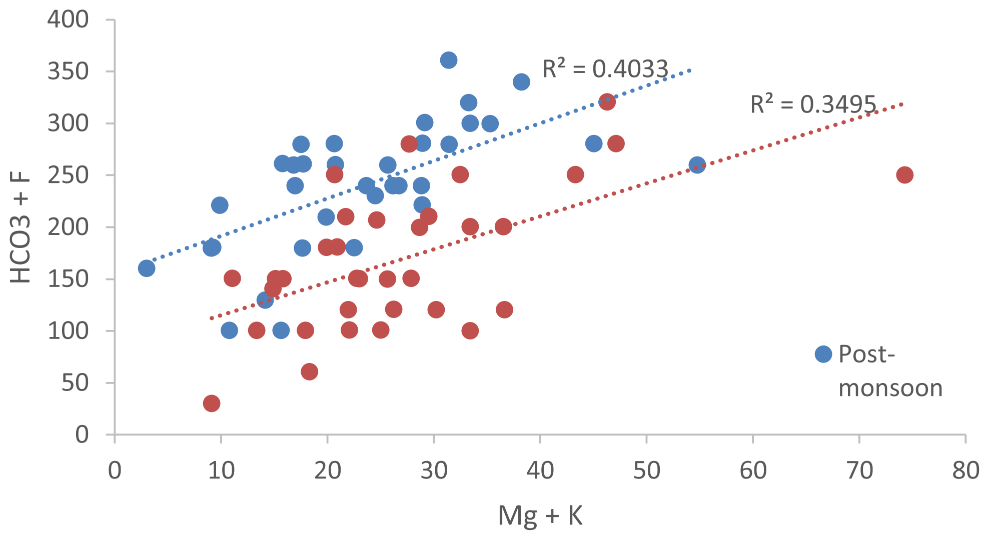

subsurface as groundwater and carrying a high content of bicarbonate and sodium ions which released comparatively more hydroxyl ions in groundwater (Fig. 5). A further exchange of ions occurs in the subsurface and results in the creation of favorable conditions to leac fluoride ions from host rocks into groundwater. The silica in the groundwater also increases with leaching of fluoride. Hornblende mineral dissociates in Na and HCO_3-rich groundwater which in turn enables leaching of fluoride from aquifer matrix. The use of agricultural fertilizers, insecticides, domestic waste water, and high withdrawal of subsurface water are another source of fluoride pollution in the aquifer system (EPA, 1997). The spatial variation maps (Fig. 6a, b) show that the PRM season has wide dispersion of elevated F concentrations in comparison with the POM season samples, having less. Furthermore, low concentrations of the F ion are observed at the upper reaches of the study area, where high precipitation resulted into high dissolution rates as well as a high dilution of the groundwater near the host basaltic geology (Kale and Pawar 2017). The downstream part of the study area has low rainfall but the presence of arable farmland results in intense agriculture with significant use of fertilizers. The fertilizers are the main cause of high concentration of F ion in that portion of the study area.

Sources of ions in the groundwater

Generally, a number of factors like natural processes, anthropogenic factors, geology and mineral composition of the area, and types of weathering are responsible for determining groundwater quality. Thus it is crucial to recognize the positive and negative assimilation within cation and anions and

Fig. 4 Correlation between the concentration of HCO_3+F vs Ca+Mg+Na

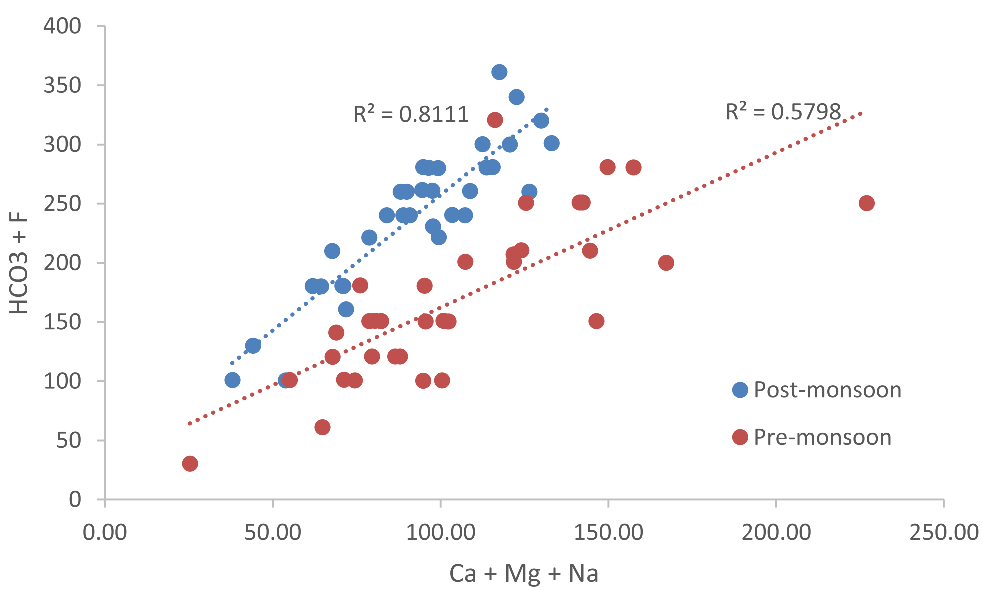

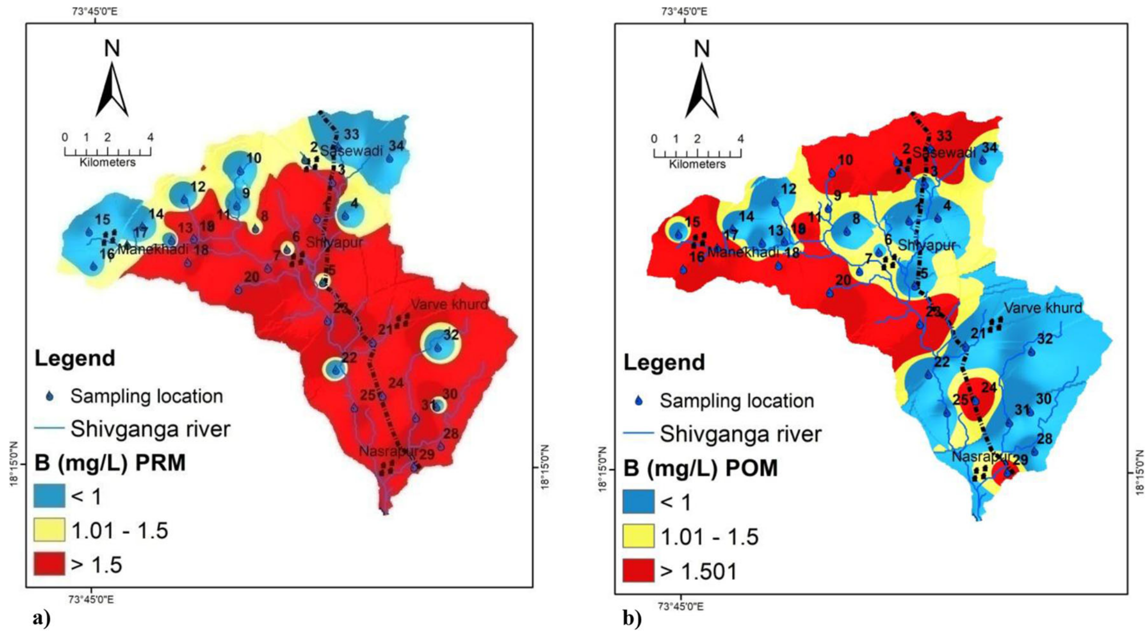

Fig. 5 Spatial distribution of boron content in the study area: **a** PRM season, **b** POM season

their combined influence on overall water quality (Wagh et al. 2020b). The ionic plot of Ca + Mg vs HCO_3 and Mg vs HCO_3 (Fig. 7a, b) represents a significant association which is indicative for weathering of olivine and pyroxene minerals (Ca + Mg–HCO_3) from host rock. The plot of Ca + Na vs HCO_3 (Fig. 7c) illustrates a positive association in both seasons which indicate some contribution is due to plagioclase dissolution. However, in the post-monsoon season, the Ca + Mg vs HCO_3 association is high due to greater rock-water contacts (Pawar et al. 2008).

Ca vs HCO_3 (Fig. 7d) plot demonstrated a good correlation and is generally used to point out calcium sources in the groundwater. The Ca is attributed to dissolution of minerals like calcite and dolomite from carbonate weathering. The geochemical plots of Ca + Mg: Cl + SO_4 (Fig. 7e) signify a positive relationship, suggestive that the groundwater may have a preference for ion pairs formation (Pawar et al. 2008; Gaikwad et al. 2020b). The plot of Ca vs Mg (Fig. 7f) indicates that about 80% of the samples are having a Ca/Mg ratio between 1 and 2, which is evidence for calcite as the main mineral (Subramani et al. 2010). Na vs HCO_3 plot indicates

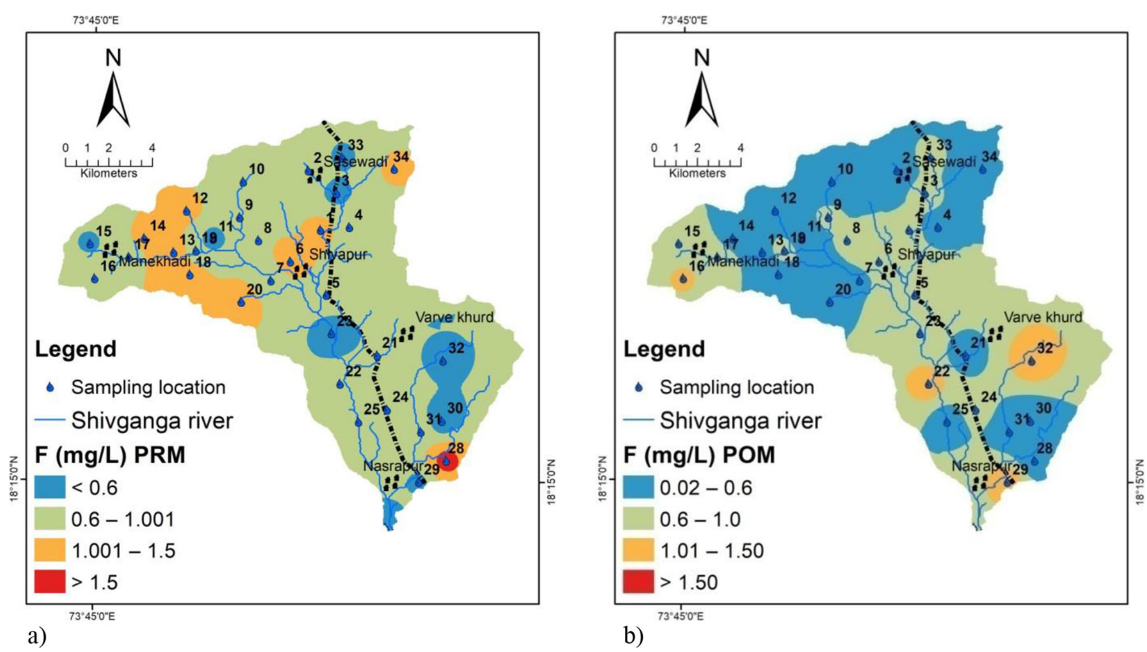

Fig. 6 Spatial distribution of fluoride content in the study area: **a** PRM season, **b** POM season

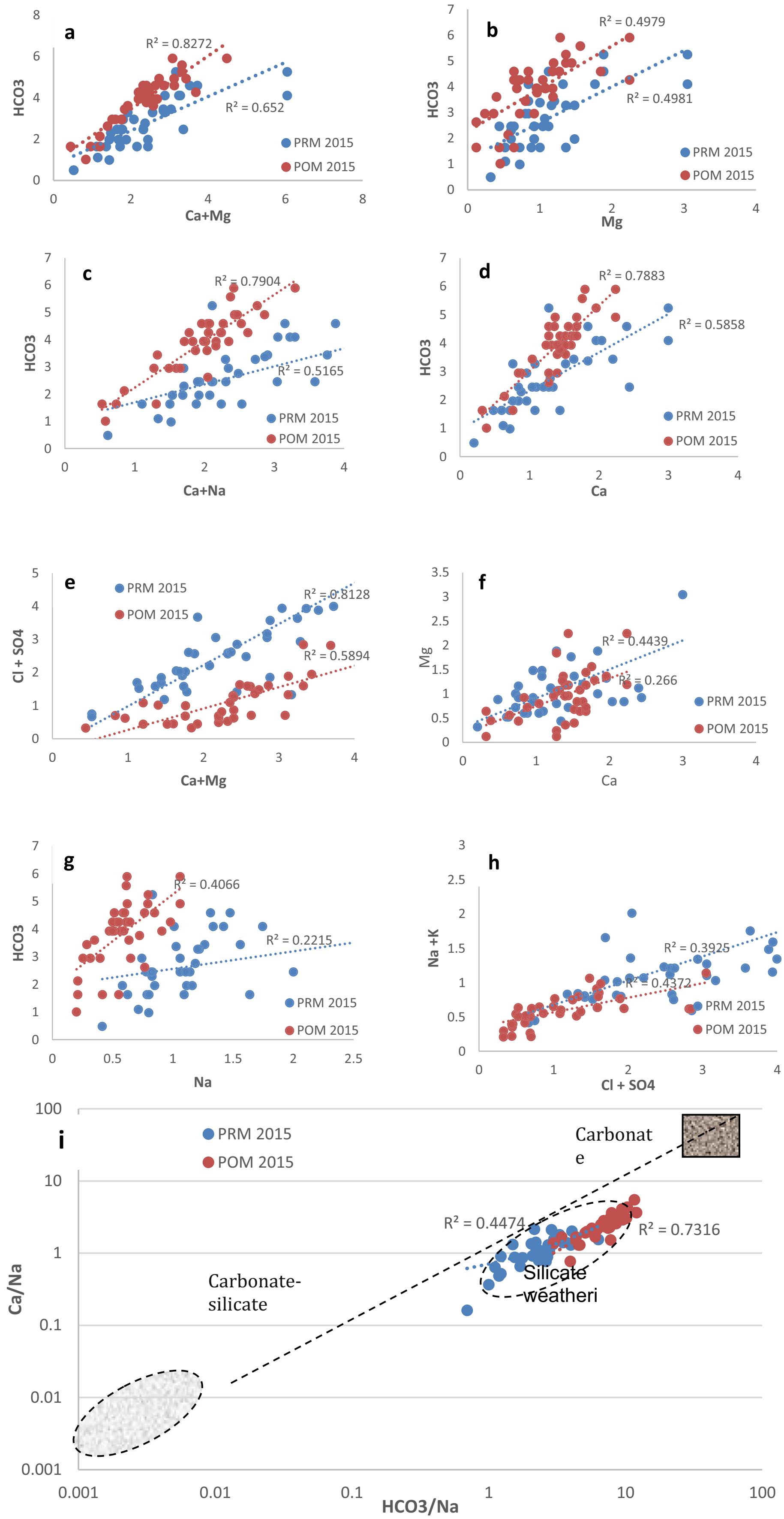
a
R² = 0.8272
R² = 0.652
PRM 2015
POM 2015
HCO3
Ca+Mg
b
R² = 0.4979
R² = 0.4981
PRM 2015
POM 2015
HCO3
Mg
c
R² = 0.7904
R² = 0.5165
PRM 2015
POM 2015
HCO3
Ca+Na
d
R² = 0.7883
R² = 0.5858
PRM 2015
POM 2015
HCO3
Ca
e
PRM 2015
POM 2015
R² = 0.8128
R² = 0.5894
Cl + SO4
Ca+Mg
f
R² = 0.4439
R² = 0.266
PRM 2015
POM 2015
Mg
Ca
g
R² = 0.4066
R² = 0.2215
PRM 2015
POM 2015
HCO3
Na
h
R² = 0.3925
R² = 0.4372
PRM 2015
POM 2015
Na +K
Cl + SO4
i
PRM 2015
POM 2015
Carbonat
e
R² = 0.4474
R² = 0.7316
Silicate
weatheri
Carbonate-
silicate
Ca/Na
HCO3/Na

◀ **Fig. 7** Relationship between the concentration of **a** Ca+Mg vs HCO_3, **b** Mg vs HCO_3, **c** Ca+Na vs HCO_3, **d** Ca vs HCO_3, **e** Ca+Mg vs Cl + SO_4, **f** Ca vs Mg, **g** Na vs HCO_3, **h** Na + K vs Cl + SO_4, **i** Ca/Na *vs* HCO_3/Na

that majority of samples shift towards HCO_3 representing groundwater derived from basalt rocks (Fig. 7g). The plot shows a good correlation between Na + K and Cl + SO_4 (Fig. 7h), representing anthropogenic pollution which appears to alter the natural groundwater composition. The bivariate plot of Ca/Na: HCO_3/Na (Fig. 7i) signifies that these ions are attributed to weathering of a silicate mineral, due to the high solubility of Na over Ca, increasing the sodium content (Wagh et al. 2019a, b). In the study area, there is little information available on groundwater geochemistry and their influence factors. However, Pawar et al. (2008) reported that the aquifers are exemplify as basalt, weathered basalt, and doleritic dyke restraining the Ca+Mg–HCO_3 water type; whereas, aquifers from alluvial parts of the study area are distinguished by the Ca+Mg+Na–HCO_3 type. The inputs of ions are mainly attributed to the weathering of silicates minerals like (olivine, augite, and plagioclase feldspar), and there is also a slight input from zeolites (Pawar et al. 2008). Groundwater quality varies in the region, due to rainwater is charged with Cl, SO_4, NO_3, Na, Ca, Mg, and small quantities of HCO_3 (Das et al. 2005). The precipitation influence in the groundwater was eliminated from the acquired geochemical data and rectified values were considered for the analyses.

Hydro-geochemical facies

Piper's trilinear diagram was used to recognize the geochemical progression in the groundwater of study region (Piper 1944). The plot represents that mixed water type Ca–Mg–Cl is dominant in most of the groundwater samples from both the seasons (Fig. 8). The plot exemplifies that alkaline earths (Ca^{2+} and Mg^{2+}) significantly go beyond the alkalis (Na^+ and K^+) and weak acids (HCO_3^- and CO_3^{2-}) and exceed the strong acids (Cl^- and SO_4^{2-}). The POM season shows the Ca+Mg–HCO_3 water type, indicating that wells are present in weathered basaltic and dolerite dyke aquifers (Pawar et al. 2008). The PRM samples show Ca–HCO_3 as well as mixed Ca + Na–HCO_3 water types that correspond to host basaltic rock lithology and anthropogenic inputs (Pawar et al. 2008). Gibb's diagram is used to evaluate processes like precipitation, rock, and evaporation dominance which control the groundwater composition in the aquifer (Gibbs 1970). It is inferred that rock dominance processes influence the groundwater quality in the studied region (Fig. 9a, b).

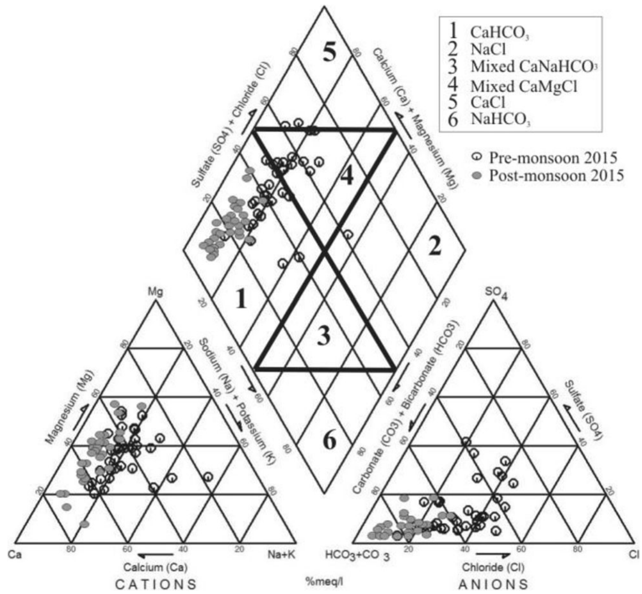

Fig. 8 Piper diagram of groundwater samples for PRM and POM seasons

Groundwater quality index

GWQI is a widely used technique to categorize the groundwater quality as excellent, good, poor, very poor, and unsuitable for drinking (Subba Rao et al. 2019, 2020). It uses the rank and weights given to the analyses parameter to calculate the groundwater quality, as it is one of the most trusted indices for the quality assessment of groundwater. GWQI values were further classified into 5 categories: excellent water quality, if GWQI value (<50); good, if GWQI values of (50 to 100); poor, if GWQI values (100 to 200); very poor, if GWQI values (200 to 300); and unsuitable water quality, if GWQI values is (>300). This classification method is used to categorize the groundwater quality in the study area. The calculated GWQI values are ranges from 35.34 to 166.53 and 38.78 to 194.47, for the PRM and the POM seasons, respectively, indicating that groundwater quality is poor to excellent for drinking. This variation may be due to the inputs of domestic and/or agricultural discharges. The POM samples exhibit poor to excellent categories of groundwater for drinking, plausibly due to agriculture return flow causing increase in boron and fluoride. The PRM has a maximum 27% samples (numbers 1, 5, 18–20, 23–25, 31) and the POM season has 15% (numbers 16, 20, 23, 29, 33) in poor category. However, only 15% of the PRM samples (numbers 9, 12–14, 16) and 18% of the POM samples (numbers 12–15, 25, 26) represent excellent (Fig. 10a, b). The central and south parts in the study area have few poor samples in the PRM season. However, in the POM season, local anthropogenic inputs resulted in poor water quality. The overall interpretation is that groundwater quality declines in the PRM season. Sample number 20 exhibited poor water quality in both the seasons and may due the proximity to agricultural field and brick kiln activities.

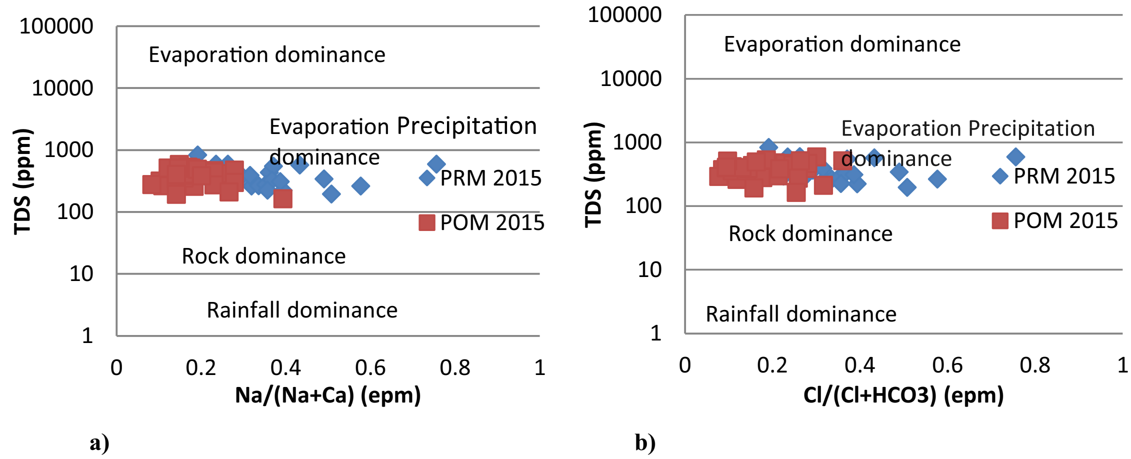

Fig. 9 Gibbs diagram: **a** Na/(Na+Ca) vs TDS, **b** Cl/(Cl+HCO3) vs TDS

Pollution index of groundwater

PIG is a numerical expression for rating the quantifying range of contamination by considering numerous parameters based on relative importance in defining groundwater quality such as pH, TDS, major cations and anions, boron, and fluoride. Several authors proposed PIG to derive the extent of contamination of surface and/or groundwater (Rao and Chaudhary 2019; Wagh et al. 2020b; Egbueri 2020; Marghade et al. 2020). The PIG values were further classified into 5 classes, namely insignificant pollution if PIG value (< 1), low pollution (1 to 1.5), moderate pollution (1.5 to 2), high pollution (2 to 2.5), and very high pollution (> 2.5). This classification method has been used to categorize the groundwater samples in the study area. The PIG values are varies with 0.44 to 1.87 with an average value of 0.83 in the PRM season, while 0.32 to 2.06 with (average 0.66) in POM season. In the present study, 34 samples for each season were studied for PIG and out of that, 2 samples (numbers 20, 31) (about 6%) found moderate pollution; 8 samples, i.e., 24% (numbers 1, 5, 18–19, 23–25, 28), were identified as low pollution; and the rest of the 24 samples, i.e., (about 70%), are showing insignificant pollution in the PRM season. In the POM season, only 1 sample (number 16) shows high pollution, 2 samples (numbers 20, 33) (about 6%) show low pollution, and the rest of the 31 sample, i.e., (about 91%), are imply insignificant pollution. This study showed that 18% of the samples are found to be unfit by PIG classification. PIG variation maps depict that southern and central parts of the study area comprise the low polluted samples in the PRM season (Fig. 11a). However, in

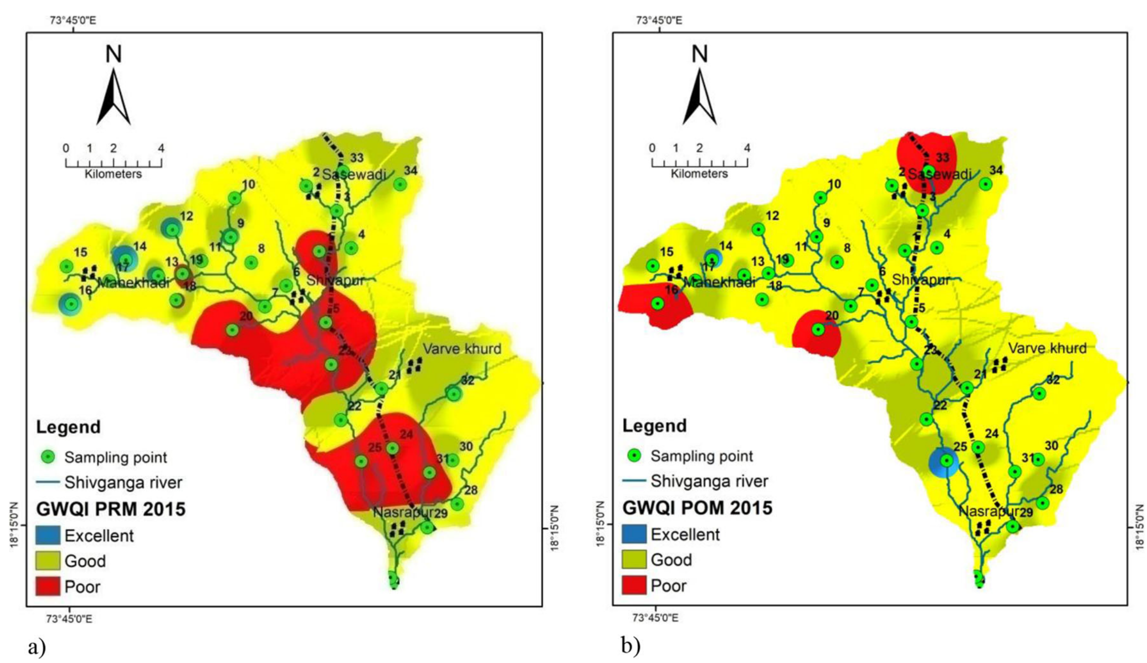

Fig. 10 Spatial distribution of the classification of GWQI for drinking purpose in **a** PRM season and **b** POM season

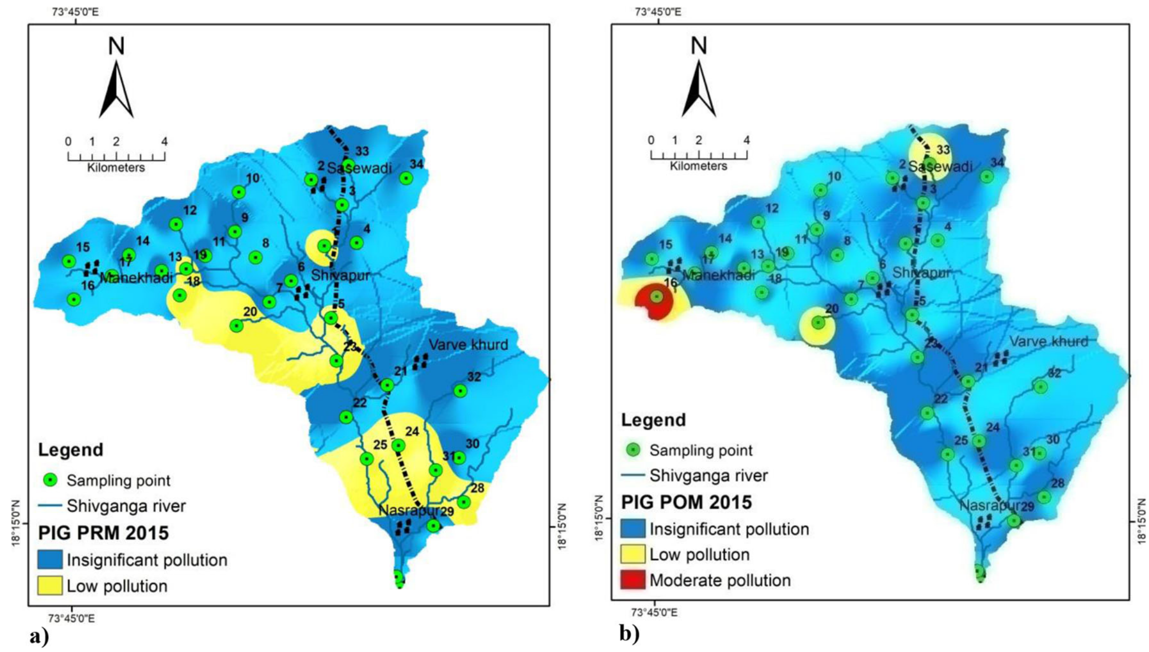

Fig. 11 Spatial distribution of PIG classification for pollution level: **a** PRM season, **b** POM season

the POM season, a few samples are found at periphery of the area having low pollution values and only one sample (number 16) showed pollution (Fig. 11b).

Human health risk assessment of fluoride and boron

In the study area, F content in groundwater above the DL (35 and 18%) in the PRM and the POM seasons and (6%) exceed the PL of WHO standards in the PRM season, thereby restricting drinking water use at a few locations. B content in (70 and 51%) surpasses the DL and 58 and 39% samples exceed the PL of the WHO in the PRM and the POM seasons, respectively. Therefore, to ascertain the human health risk, B and F were considered. The EDI values of F for different age groups which varied for inhabitants show that infants (less than 0.5 years) are having high ingestion groundwater with high F content as compared with children and adults as the body mass will be less for children. It is exemplify that 41% of the samples in the PRM season and 8% of the samples in the POM season are above the safe limit of F, 0.03 mg/kg/day for infants. The safe EDI value for children is 0.13 mg/kg/day for F, where all samples are below than that except 1 sample in the PRM season, while adults have a safe limit of 0.05 mg/kg/day; 29% of the samples in the PRM season and 12% of the samples in the POM season exceeded this limit. If HQ value of F is greater than 1, then it signifies that people are exposed to non-carcinogenic health risks associated with high F content in the drinking water (Tables 5 and 6). In the study area, HQ values of F vary from 0.09 to 1.60, 0.13 to 2.46, and 0.06 to 1.11 in the PRM season and 0.02 to 5.75, 0.03 to 8.84, and 0.01 to 3.99 in the POM season for adults, children, and infants, respectively. The children age group shows more risk than infants and adults. The probable cause for the HHRA for children is the modest body weight (Bw) as comparison with other age groups (Zango et al. 2019). HHRA results confirm that non carcinogenic health risk of F is in order of children > adults > infants. The children age group is highly vulnerable to potential of dental and skeletal deformities in the future.

In the study area, EDI value of B ranges from 0.0 to 0.65, 0.0 to 1.00, and 0.0 to 0.45 for adults, children, and infants, respectively, in the PRM season (Table 5), while 0.0 to 0.75, 0.0 to 1.15, and 0.0 to 0.52 for adults, children, and infants, respectively, in the POM season (Table 6). The results show that the POM season has a lower health risk as B concentration decreases due to dilution phenomenon in the POM season as compared with the PRM season. Infants and children are having high ingestion rates of groundwater with high B content as compared with adults as the body mass of the younger population will be less. Also, 68% samples from the PRM season and 53% from the POM season are above the safe limit of 0.01 mg/kg/day of B for infants (Tables 5 and 6). The PRM season (38%) and the POM season (32%) samples are having values higher than that safe EDI value of (0.16 mg/kg/day) for children in both seasons. If, HQ value for B is greater than 1, it signifies that the people are more vulnerable to non-carcinogenic health-related problems (Tables 5 and 6). The HQ values ranges from 0.00 to 5.00, 0.01 to 7.68, and 0.0 to 3.47 in the PRM season for adults, children, and infants, respectively (Table 5), although HQ values in the POM season vary from 0.02 to 5.75, 0.03 to 8.84, and 0.01 to 3.99 for adults, children, and infants, respectively (Table 6). The highest HQ values were found in children, compared to lower value associated with adults and infants.

Table 5 Values of EDI, HQ, and THI for different age groups in the PRM season

Sr no..	Adults					Children					Infants				
	EDI F	HQ F	EDI B	HQ B	THI	EDI F	HQ F	EDI B	HQ B	THI	EDI F	HQ F	EDI B	HQ B	THI
1	0.06	1.02	0.29	2.24	3.26	0.09	1.56	0.45	2.63	4.20	0.04	0.71	0.20	1.56	2.26
2	0.05	0.84	0.08	0.59	1.44	0.08	1.30	0.12	0.91	2.21	0.04	0.59	0.05	0.41	1.00
3	0.02	0.34	0.09	0.72	1.06	0.03	0.52	0.14	1.20	1.72	0.01	0.24	0.06	0.50	0.73
4	0.04	0.67	0.00	0.00	0.67	0.06	1.03	0.00	0.52	1.55	0.03	0.46	0.00	0.00	0.47
5	0.05	0.90	0.06	0.46	1.35	0.08	1.38	0.09	1.30	2.67	0.04	0.62	0.04	0.32	0.94
6	0.07	1.12	0.05	0.39	1.51	0.10	1.72	0.08	0.40	2.13	0.05	0.78	0.03	0.27	1.05
7	0.03	0.55	0.22	1.71	2.26	0.05	0.84	0.34	1.31	2.15	0.02	0.38	0.15	1.19	1.57
8	0.05	0.83	0.06	0.49	1.33	0.08	1.28	0.10	0.78	2.06	0.03	0.58	0.04	0.34	0.92
9	0.05	0.81	0.00	0.00	0.81	0.07	1.24	0.00	0.01	1.25	0.03	0.56	0.00	0.00	0.56
10	0.03	0.54	0.03	0.22	0.76	0.05	0.83	0.04	0.01	0.84	0.02	0.37	0.02	0.15	0.53
11	0.01	0.23	0.08	0.63	0.85	0.02	0.35	0.13	0.52	0.87	0.01	0.16	0.06	0.43	0.59
12	0.06	1.07	0.00	0.00	1.07	0.10	1.64	0.00	0.01	1.65	0.04	0.74	0.00	0.00	0.75
13	0.08	1.36	0.00	0.00	1.36	0.13	2.09	0.00	0.01	2.09	0.06	0.94	0.00	0.00	0.94
14	0.06	0.98	0.00	0.00	0.99	0.09	1.51	0.00	0.40	1.91	0.04	0.68	0.00	0.00	0.69
15	0.03	0.45	0.00	0.00	0.46	0.04	0.70	0.00	0.01	0.70	0.02	0.31	0.00	0.00	0.32
16	0.05	0.84	0.05	0.35	1.19	0.08	1.30	0.07	1.00	2.29	0.04	0.59	0.03	0.24	0.83
17	0.04	0.70	0.05	0.40	1.10	0.06	1.07	0.08	0.55	1.62	0.03	0.48	0.04	0.28	0.76
18	0.07	1.17	0.29	2.26	3.42	0.11	1.79	0.45	2.20	3.99	0.05	0.81	0.20	1.57	2.38
19	0.03	0.51	0.45	3.49	4.00	0.05	0.79	0.70	4.04	4.82	0.02	0.36	0.32	2.42	2.78
20	0.07	1.13	0.65	5.00	6.13	0.10	1.74	1.00	5.27	7.01	0.05	0.79	0.45	3.47	4.25
21	0.03	0.54	0.11	0.85	1.39	0.05	0.83	0.17	0.33	1.16	0.02	0.37	0.08	0.59	0.97
22	0.04	0.70	0.00	0.00	0.71	0.06	1.08	0.00	0.55	1.63	0.03	0.49	0.00	0.00	0.49
23	0.01	0.18	0.31	2.40	2.58	0.02	0.28	0.48	3.78	4.06	0.01	0.13	0.22	1.67	1.79
24	0.05	0.89	0.37	2.83	3.72	0.08	1.36	0.57	1.30	2.66	0.04	0.62	0.26	1.96	2.58
25	0.04	0.69	0.41	3.16	3.85	0.06	1.06	0.63	2.59	3.65	0.03	0.48	0.29	2.20	2.67
26	0.06	0.97	0.25	1.90	2.87	0.09	1.48	0.38	3.78	5.26	0.04	0.67	0.17	1.32	1.99
27	0.01	0.09	0.09	0.71	0.80	0.01	0.13	0.14	1.10	1.23	0.00	0.06	0.06	0.49	0.55
28	0.10	1.60	0.21	1.64	3.24	0.15	2.46	0.33	1.33	3.79	0.07	1.11	0.15	1.14	2.25
29	0.03	0.46	0.15	1.16	1.62	0.04	0.71	0.23	2.14	2.85	0.02	0.32	0.10	0.81	1.13
30	0.01	0.17	0.00	0.03	0.21	0.02	0.27	0.01	0.01	0.27	0.01	0.12	0.00	0.02	0.14
31	0.05	0.78	0.60	4.64	5.42	0.07	1.20	0.93	7.68	8.89	0.03	0.54	0.42	3.22	3.77
32	0.02	0.41	0.00	0.00	0.41	0.04	0.63	0.00	0.48	1.11	0.02	0.28	0.00	0.00	0.29
33	0.03	0.47	0.00	0.00	0.47	0.04	0.72	0.00	0.40	1.12	0.02	0.33	0.00	0.00	0.33
34	0.06	0.94	0.00	0.00	0.94	0.09	1.44	0.00	0.01	1.45	0.04	0.65	0.00	0.00	0.65
Min.	0.01	0.09	0.00	0.00	0.21	0.01	0.13	0.00	0.01	0.27	0.00	0.06	0.00	0.00	0.14
Max.	0.10	1.60	0.65	5.00	6.13	0.15	2.46	1.00	7.68	8.89	0.07	1.11	0.45	3.47	4.25
Avg.	0.04	0.73	0.15	1.13	1.86	0.07	1.13	0.23	1.43	2.55	0.03	0.51	0.10	0.78	1.29

Table 6 Values of EDI, HQ, and THI for different age groups in the POM season

Sr no.	Adults					Children					Infants				
	EDI F	HQ F	EDI B	HQ B	THI	EDI F	HQ F	EDI B	HQ B	THI	EDI F	HQ F	EDI B	HQ B	THI
1	0.03	0.56	0.00	0.00	0.56	0.03	0.86	0.00	0.01	0.86	0.02	0.39	0.00	0.00	0.39
2	0.02	0.34	0.16	1.21	1.55	0.02	0.52	0.24	1.86	2.38	0.01	0.24	0.11	0.84	1.08
3	0.04	0.62	0.03	0.22	0.83	0.04	0.95	0.04	0.33	1.28	0.03	0.43	0.02	0.15	0.58
4	0.03	0.44	0.02	0.14	0.58	0.03	0.68	0.03	0.21	0.89	0.02	0.31	0.01	0.09	0.4
5	0.05	0.89	0.00	0.00	0.89	0.05	1.36	0.00	0.01	1.37	0.04	0.62	0.00	0.00	0.62
6	0.04	0.75	0.05	0.39	1.13	0.04	1.15	0.08	0.59	1.74	0.03	0.52	0.03	0.27	0.79
7	0.03	0.44	0.05	0.38	0.82	0.03	0.68	0.08	0.59	1.27	0.02	0.31	0.03	0.26	0.57
8	0.03	0.57	0.00	0.00	0.58	0.03	0.88	0.00	0.01	0.89	0.02	0.40	0.00	0.00	0.4
9	0.04	0.63	0.08	0.59	1.22	0.04	0.98	0.12	0.91	1.88	0.03	0.44	0.05	0.41	0.85
10	0.01	0.16	0.11	0.88	1.04	0.01	0.24	0.18	1.36	1.60	0.01	0.11	0.08	0.61	0.72
11	0.01	0.22	0.12	0.92	1.14	0.01	0.33	0.18	1.42	1.75	0.01	0.15	0.08	0.64	0.79
12	0.02	0.37	0.00	0.00	0.37	0.02	0.56	0.00	0.01	0.57	0.02	0.25	0.00	0.00	0.25
13	0.02	0.40	0.00	0.00	0.40	0.02	0.61	0.00	0.01	0.62	0.02	0.28	0.00	0.00	0.28
14	0.01	0.23	0.00	0.00	0.24	0.01	0.36	0.00	0.01	0.37	0.01	0.16	0.00	0.00	0.16
15	0.04	0.60	0.00	0.00	0.60	0.04	0.92	0.00	0.01	0.93	0.03	0.42	0.00	0.00	0.42
16	0.06	0.96	0.75	5.75	6.71	0.06	1.47	1.15	8.84	10.31	0.04	0.66	0.52	3.99	4.65
17	0.05	0.90	0.18	1.38	2.27	0.05	1.38	0.28	2.12	3.49	0.04	0.62	0.12	0.96	1.58
18	0.01	0.23	0.14	1.09	1.32	0.01	0.36	0.22	1.67	2.03	0.01	0.16	0.10	0.76	0.92
19	0.05	0.77	0.00	0.00	0.77	0.05	1.18	0.00	0.01	1.18	0.03	0.53	0.00	0.00	0.53
20	0.02	0.34	0.39	2.98	3.32	0.02	0.52	0.60	4.58	5.11	0.01	0.24	0.27	2.07	2.31
21	0.01	0.24	0.00	0.00	0.25	0.01	0.37	0.00	0.01	0.38	0.01	0.17	0.00	0.00	0.17
22	0.07	1.17	0.00	0.00	1.18	0.07	1.80	0.00	0.01	1.81	0.05	0.82	0.00	0.00	0.82
23	0.04	0.67	0.29	2.24	2.91	0.04	1.03	0.45	3.44	4.47	0.03	0.46	0.20	1.56	2.02
24	0.04	0.67	0.16	1.24	1.91	0.04	1.03	0.25	1.90	2.93	0.03	0.46	0.11	0.86	1.32
25	0.02	0.25	0.03	0.26	0.52	0.02	0.39	0.05	0.41	0.79	0.01	0.18	0.02	0.18	0.36
26	0.04	0.75	0.06	0.44	1.19	0.04	1.15	0.09	0.67	1.82	0.03	0.52	0.04	0.30	0.82
27	0.05	0.81	0.00	0.00	0.81	0.05	1.24	0.00	0.01	1.25	0.03	0.56	0.00	0.00	0.56
28	0.01	0.17	0.00	0.00	0.17	0.01	0.25	0.00	0.01	0.26	0.01	0.11	0.00	0.00	0.11
29	0.07	1.22	0.11	0.83	2.05	0.07	1.87	0.17	1.28	3.15	0.05	0.85	0.08	0.58	1.43
30	0.01	0.16	0.00	0.00	0.16	0.01	0.24	0.00	0.01	0.25	0.01	0.11	0.00	0.00	0.11
31	0.02	0.30	0.00	0.00	0.31	0.02	0.47	0.00	0.01	0.47	0.01	0.21	0.00	0.00	0.21
32	0.08	1.29	0.00	0.00	1.29	0.08	1.98	0.00	0.01	1.98	0.05	0.89	0.00	0.00	0.89
33	0.04	0.62	0.38	2.92	3.54	0.04	0.95	0.58	4.49	5.44	0.03	0.43	0.26	2.03	2.46
34	0.00	0.02	0.02	0.15	0.17	0.00	0.03	0.03	0.23	0.26	0.00	0.01	0.01	0.11	0.12
Min.	0.00	0.02	0.00	0.00	0.02	0.00	0.03	0.00	0.01	0.03	0.00	0.01	0.00	0.00	0.11
Max.	0.08	5.75	0.75	7.04	1.98	0.08	8.84	1.15	10.82	0.89	0.05	3.99	0.52	4.89	4.65
Avg.	0.03	0.71	0.09	1.26	0.85	0.03	1.09	0.14	1.94	0.38	0.02	0.49	0.06	0.87	0.87

Fig. 12 THI classification in percentage for adults, children, and infants for both seasons

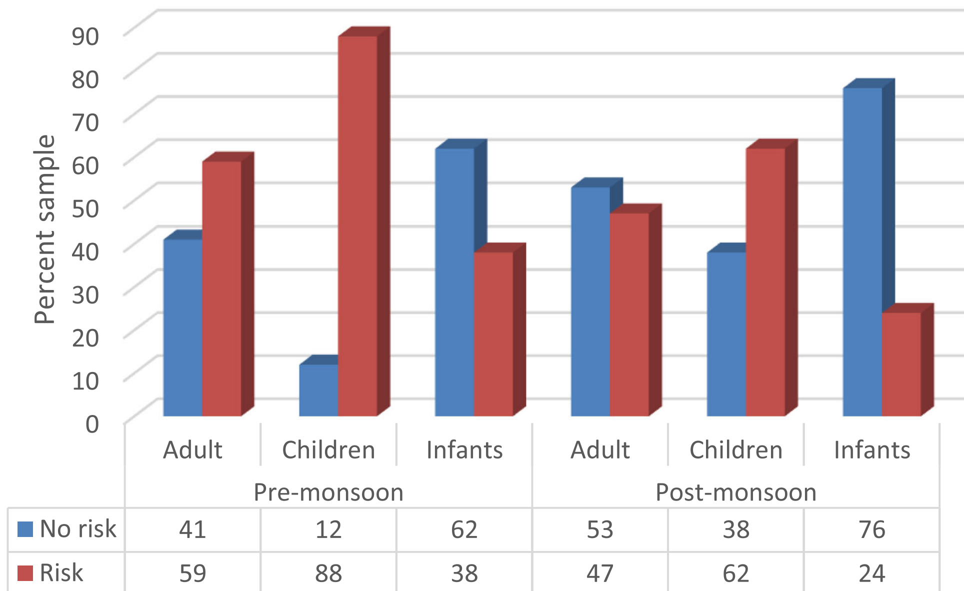

Total hazard index (THI) is computed from summation of the hazard quotient (HQs) of B and F; if THI is more than 1 it means, the water probably caused health problems in relation to a non carcinogenic risk; while if the value is less than 1, it indicates there are no symptoms of non-carcinogenic risk (USEPA 2014). THI value was calculated separately for the adults, children, and infants, given in the Tables 5 and 6. THI values ranged from 0.21 to 6.13 (avg. 1.86), 0.27 to 8.89 (avg. 2.55), and 0.14 to 4.25 (avg. 1.29) for adults, children, and infants, respectively, in the PRM season (Table 5). Children (88%), adults (59%), and infants (38%) possess non-carcinogenic risk as THI values (>1) in the PRM season (Fig. 12), while in the POM season, THI value varies for adults: 0.02 to 6.71 (avg. 1.26); children: 0.03 to 10.3(avg. 11.94); and infants: 0.01 to 3.99 (avg. 0.49) (Table 6). THI result inferred that about 62% children, 47% adults, and 24% of infants are possessed to non-carcinogenic risk in the POM season (Fig. 12). It is shown that children face higher non-carcinogenic health risk than infants and adults and small body mass compared to adults.

The spatial variation maps of THI for infants in the PRM and POM seasons are shown (Fig. 13a, b). Figure 14a shows the complete northern part of the study area is identified under the no risk category; however, central and south parts of the

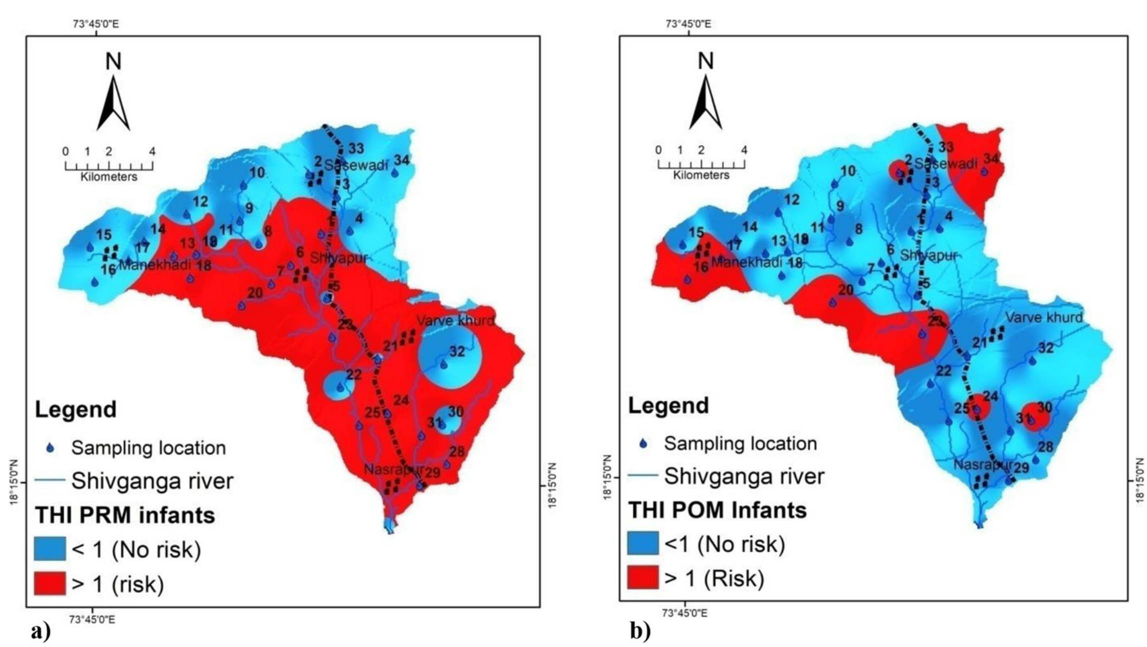

Fig. 13 Spatial distribution THI for infants: **a** PRM season, **b** POM season

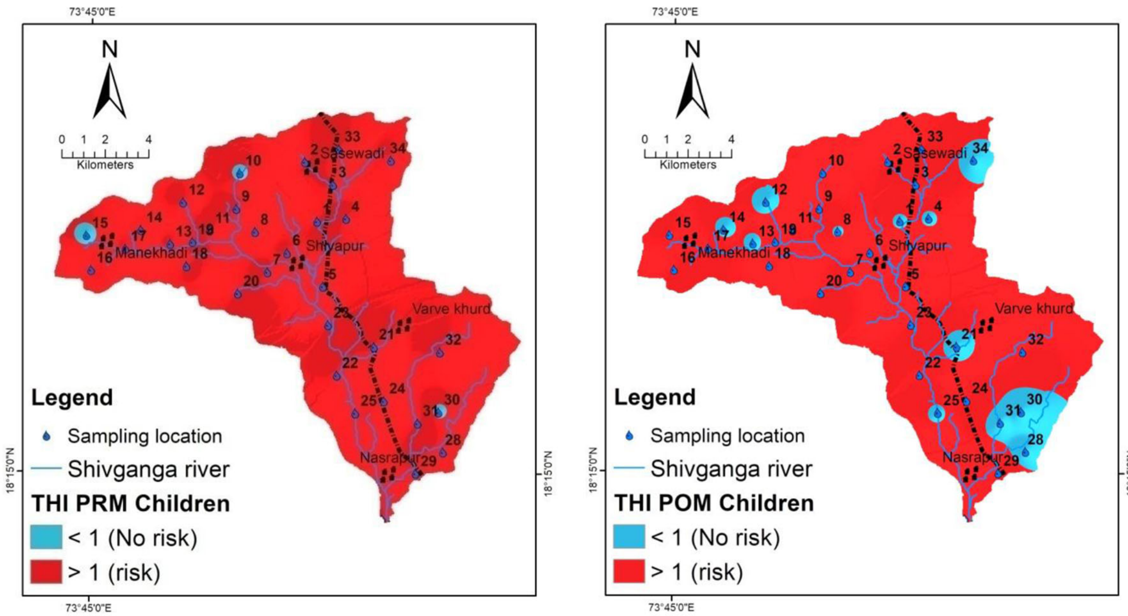

a) b)

Fig. 14 Spatial distribution of THI for children: **a** PRM season, **b** POM season

study area fall in the higher risk category (except sample numbers 22, 28, 31). Figure 13b shows that in POM season, the locations for sample numbers 2, 16, 20, 23, 24, 30, 31, and 34 have a potential for a health risk. It is inferred that infants are more vulnerable to health risk in the PRM season. The spatial extent of THI for children (Fig. 14a, b) demonstrate that the PRM season (samples numbers 10, 15, 31) and the POM season (numbers 6, 12, 14, 21, 26, 29, 31, 32) confirm that their fitness for drinking and remaining samples from both seasons is unfit for drinking use. For adult risk, many of the samples showed a potential for exposed risk except sample numbers (4, 9, 10, 15, 22, 28, 31, and 34) in the PRM season. However, in the POM season, the samples (numbers 4, 8, 12-15, 21, 25, 28, 29, 31, 32) fall in no risk category, while other samples showed potential health risk for adults (Fig. 15a, b). The POM season groundwater quality is comparatively better than the PRM season. During the POM season, the concentration of ions has decreased due to dilution by fresh rainwater recharge in the aquifer system; therefore, in PRM season, the inhabitants are more prone to HHRA. HHRA results showed that children have a greater non-carcinogenic risk than adults and infants in both seasons.

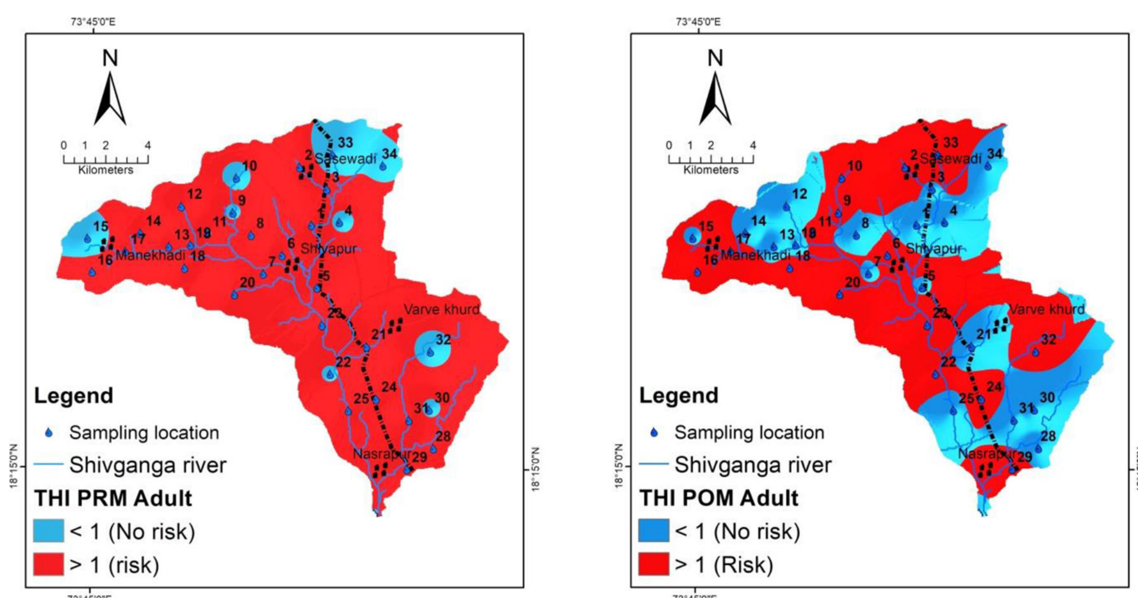

a) b)

Fig. 15 Spatial distribution THI for adults: **a** PRM season, **b** POM season

Conclusions

The study is summarized with the following conclusions, inferences drawn from hydro-chemical analysis, GWQI, PIG, and HHRA from the Shivganga River basin of Western India. Hydro-chemical interpretation reveals that the groundwater quality is slightly alkaline with hard to very hard water types. As per the WHO drinking standards, the parameters like pH, Na^+, K^+, Cl^-, SO_4^-, and NO_3^- are within threshold limits. Besides, EC (80 and 68%), TDS (24 and 15%), TH (95 and 97%), Ca^{2+} (18 and 6%), Mg^{2+} (3%), and HCO_3^- (30 and 76%) surpass the desirable limits in the PRM and the POM seasons, respectively. High contents of EC and TDS were observed in the downstream part of the study area due to accrual of salt. TH is increased in the POM season due to dissolution of minerals, thereby groundwater is unsuitable for drinking. F content in groundwater above the DL (35 and 18%) in the PRM and the POM seasons and (6%) exceed the PL of WHO standards in the PRM season. B content in (70 and 51%) surpasses the DL and 58 and 39% samples exceed the PL of the WHO in the PRM and the POM seasons respectively, thus restricted drinking water use at a few locations. The enrichment of B content in groundwater is due to sewage effluent, fertilizers application, agricultural runoff, overuse of herbicides, and poultry waste in the basin. The excessive F is due to semi-arid condition which increased the F ion leaching from the host lithology. Also, the minerals like fluorite, muscovite, and biotite are the main contributors for leaching of F ion in the groundwater. In addition, the slight alkaline nature of groundwater is more favorable to dissolve the fluorite mineral. GWQI classification exemplified that 27 and 15% samples fall in poor category and only 15 and 18% samples into excellent category from PRM and the POM seasons, respectively. PIG results classified groundwater samples as 6% moderate pollution, 24% low pollution, and 70% insignificant pollution in the PRM season. Also, 3% signify high pollution, 6% low pollution, and 91% insignificant pollution in POM season. Consequently, 18% of groundwater samples are unfit for drinking. The HQ of F inferred that children have a higher risk than adults and infants. HHRA results corroborate that non carcinogenic risk of F in order of children > adults > infants. Therefore, children are more susceptible to non carcinogenic risk with deformities of dental- and skeletal-related F problem than other age groups. The average HQ of B shows the order of impacts with children > adults > infants suggesting that children are the most vulnerable age group. THI results show (88 and 62%) children, (59 and 47%) adults, and (38 and 24%) infants in the PRM and POM seasons respectively possess non-carcinogenic risk as THI values (>1). Thus, the remedial measures like use of safe drinking water, de-fluoridation techniques, intake of calcium- and phosphorous-rich food, least use B-herbicides and manures, poultry waste management, and public awareness on health risk of F and B contamination are recommended to reduce the health problems in the study area.

Supplementary Information The online version contains supplementary material available at https://doi.org/10.1007/s11356-021-15554-2.

Acknowledgements The authors express their sincere thanks to Head, Department of Environmental Science, Savitribai Phule, Pune University, Pune, for providing necessary facilities to carry out the present research. Also, authors thank to editor and reviewers for their meaningful suggestions and comments which helps to strengthen the manuscript quality in more scientific approach.

Author contribution Ajaykumar Kadam: conceptualization, data collection and analysis.

Vasant Wagh: assist in manuscript writing and interpretation of data.

James Jacobs: assist in manuscript writing and correct English language and grammatical errors.

Sanjay Patil: helps in data interpretation.

Namdev Pawar: helps in interpretation of data.

Bhavana Umrikar: supervision of research and assist in field work.

Rabindranath Sankhua: supervision of the research and assist in field work.

Suyash Kumar: assist in writing geology of the area.

Data availability Not applicable.

Declarations

Ethics approval Not applicable to this manuscript.

Consent to participate Not applicable.

Consent to publish Not applicable

References

Adimalla N (2019a) Controlling factors and mechanism of groundwater quality variation in semiarid region of South India: an approach of water quality index (WQI) and health risk assessment (HRA). Environ Geochem Health 42:1725–1752. https://doi.org/10.1007/s10653-019-00374-8

Adimalla N (2019b) Groundwater quality for drinking and irrigation purposes and potential health risks assessment: a case study from semi-arid region of South India. Expo Health 11(2):109–123

Adimalla N, Li P, Venkatayogi S (2018) Hydrogeochemical evaluation of groundwater quality for drinking and irrigation purposes and integrated interpretation with water quality index studies. Environ Process 5(2):363–383

Adimalla N, Qian H, Nandan MJ (2020) Groundwater chemistry integrating the pollution index of groundwater and evaluation of potential

human health risk: A case study from hard rock terrain of south India. Ecotoxicol Environ Saf 206:111217. https://doi.org/10.1016/j.ecoenv.2020.111217
Ahmad W, Zia MH, Malhi SS, Niaz A, Ullah S (2012) Boron deficiency in soils and crops: a review. Crop Plant 2012:65–97
APHA (2005) Standard methods for the examination of water and wastewater, 21st edn. American Public Health Association, New York
Balamurugan P, Kumar PS, Shankar K, Nagavinothini R, Sajil Kumar PJ (2020) Impact of climate and anthropogenic activities on groundwater quality for domestic and irrigation purposes in Attur region, Tamilnadu, India. Desalin Water Treat 208:172–195
Berner EK, Berner RA (1987) The global water cycle: geochemistry environment (No. 551.49 B47)
Bhat MA, Wani AS, Vijay K, Jyotirmaya S, Dinesh T (2018) An overview of the assessment of groundwater quality for irrigation. J Agri Sci Food Res 9:209
Brindha K, Pavelic P, Sotoukee T, Douangsavanh S, Elango L (2017) Geochemical characteristics and groundwater quality in the Vientiane Plain, Laos. Exposure and Health 9(2):89–104. https://doi.org/10.1007/s12403-016-0224-8
Census of India (2011). http://www.census2011.co.in/data/town/802819-bhor-maharashtra.html. Accessed Aug 2012
CGWB (2013) Central Groundwater Board. Available from http://cgwb.gov.in/district_profile/maharashtra/Pune.pdf
CGWB Report (2010) Unpublished report on ground water resources and development potentials of Pune district, Maharashtra
Chen J, Wu H, Qian H, Gao Y (2017) Assessing nitrate and fluoride contaminants in drinking water and their health risk of rural residents living in a semiarid region of Northwest China. Expo Health 9(3): 183–195
Das S, Nag SK (2017) Application of multivariate statistical analysis concepts for assessment of hydrogeochemistry of groundwater—a study in Suri I and II blocks of Birbhum District, West Bengal, India. Appl Water Sci 7(2):873–888
Das A, Krishnaswami S, Sarin MM, Pande K (2005) Chemical weathering in the Krishna Basin and Western Ghats of the Deccan Traps, India: rates of basalt weathering and their controls. Geochim Cosmochim Acta 69:2067–2084. https://doi.org/10.1016/j.gca.2004.10.014
Egbueri JC (2020) Groundwater quality assessment using pollution index of groundwater (PIG), ecological risk index (ERI) and hierarchical cluster analysis (HCA): a case study. Groundw Sustain Dev 10: 100292
Gaikwad SK, Kadam AR, Ramgir RR, Kashikar AS, Wagh VM, Kandekar AM, ..., Kamble KD (2020a) Assessment of the groundwater geochemistry from a part of west coast of India using statistical methods and water quality index. HydroResearch 3:48–60. https://doi.org/10.1016/j.hydres.2020.04.001
Gaikwad S, Gaikwad S, Meshram D, Wagh V, Kandekar A, Kadam A (2020b) Geochemical mobility of ions in groundwater from the tropical western coast of Maharashtra, India: implication to groundwater quality. Environ Dev Sustain 22(3):2591–2624
Gibbs RJ (1970) Mechanisms controlling world water chemistry. Science 170(3962):1088–1090
Haji M, Karuppannan S, Qin D, Shube H, Kawo NS (2021) Potential human health risks due to groundwater fluoride contamination: a case study using multi-techniques approaches (GWQI, FPI, GIS, HHRA) in Bilate River Basin of Southern Main Ethiopian Rift, Ethiopia. Arch Environ Contam Toxicol 80(1):277–293
Haritash AK, Kaushik CP, Kaushik A (2008) Suitability assessment of groundwater for drinking, irrigation and industrial use in some North Indian villages. Environ Monit Assess 145:397–406. https://doi.org/10.1007/s10661-007-0048-x
He X, Li P, Wu J, Wei M, Ren X, Wang D (2020) Poor groundwater quality and high potential health risks in the Datong basin, northern China: research from published data. Environ Geochem Health 43: 791–812. https://doi.org/10.1007/s10653-020-00520-7
ICMR (Indian Council of Medical Research) Expert Group (1990) Nutrient requirements and recommended dietary allowances for Indians: a report of the Expert Group of the Indian Council of Medical Research. Indian Council of Medical Research, New Delhi
Kadam A, Karnewar AS, Umrikar B, Sankhua RN (2018) Hydrological response-based watershed prioritization in semiarid, basaltic region of western India using frequency ratio, fuzzy logic and AHP method. Environ Dev Sustain 21:1809–1833. https://doi.org/10.1007/s10668-018-0104-4
Kadam A, Wagh V, Umrikar B, Sankhua R (2020) An implication of boron and fluoride contamination and its exposure risk in groundwater resources in semi-arid region, Western India. Environ Dev Sustain 22(7):7033–7056. https://doi.org/10.1007/s10668-019-00527-w
Kadam A, Wagh V, Patil S, Umrikar B, Sankhua R, Jacobs J (2021a) Seasonal variation in groundwater quality and beneficial use for drinking, irrigation, and industrial purposes from Deccan Basaltic Region, Western India. Environ Sci Pollut Res 28(20):26082–26104
Kadam A, Wagh V, Patil S, Umrikar B, Sankhua R (2021b) Seasonal assessment of groundwater contamination, health risk and chemometric investigation for a hard rock terrain of western India. Environ Earth Sci 80(5):1–22
Kale S, Pawar NJ (2017) Fluoride accumulation in groundwater from semi-arid part of Deccan Volcanic Province, India: a cause of urolithiasis outbreak. Hydrospatial Anal 1:9–17. https://doi.org/10.21523/gcj3.17010102
Kale SS, Kadam AK, Kumar S, Pawar NJ (2010) Evaluating pollution potential of leachate from landfill site, from the Pune metropolitan city and its impact on shallow basaltic aquifers. Environ Monit Assess 162:327–346. https://doi.org/10.1007/s10661-009-0799-7
Kawo NS, Karuppannan S (2018) Groundwater quality assessment using water quality index and GIS technique in Modjo River Basin, central Ethiopia. J Afr Earth Sci 147:300–311
Kumar S, Shirke KD, Pawar NJ (2008) GIS-based colour composites and overlays to delineate heavy metal contamination zones in the shallow alluvial aquifers, Ankaleshwar industrial estate, south Gujarat, India. Environ Geol 54:117–129. https://doi.org/10.1007/s00254-007-0799-2
Ledesma-ruiz R, Mahlknecht J, Ramos-leal JA (2016) Rock–water interactions and pollution processes in the volcanic aquifer system of Guadalajara, Mexico, using inverse geochemical modeling. Appl Geochem 68:79–94
Li P, Li X, Meng X, Li M, Zhang Y (2016) Appraising groundwater quality and health risks from contamination in a semiarid region of northwest China. Exposure and Health 8(3):361–379
Locsey KL, Cox ME (2003) Statistical and hydrochemical methods to compare basalt- and basement rock-hosted groundwaters: Atherton Tablelands, north-eastern Australia. Environ Geol 43:698–713. https://doi.org/10.1007/s00254-002-0667-z
Marghade D, Malpe DB, Subba Rao N, Sunitha B (2020) Geochemical assessment of fluoride enriched groundwater and health implications from a part of Yavtmal District, India. Hum Ecol Risk Assess Int J 26(3):673–694
Matthess G (1982) The properties of groundwater. (No. 551.49 M38). Wiley, New York
Mukate S, Panaskar D, Wagh V, Muley A, Jangam C, Pawar R (2017) Impact of anthropogenic inputs on water quality in Chincholi industrial area of Solapur, Maharashtra, India. Groundw Sustain Dev 7: 359–371. https://doi.org/10.1016/j.gsd.2017.11.001
Mukate S, Wagh V, Panaskar D, Jacobs JA, Sawant A (2019) Development of new integrated water quality index (IWQI) model to evaluate the drinking suitability of water. Ecol Indic 101:348–354
Mukate SV, Panaskar DB, Wagh VM, Baker SJ (2020) Understanding the influence of industrial and agricultural land uses on groundwater

quality in semiarid region of Solapur, India. Environ Dev Sustain 22(4):3207–3238

Narsimha A, Li P (2019) Occurrence, health risks and geochemical mechanisms of fluoride and nitrate in groundwater of the rock-dominant semi-arid region, Telangana State, India. Hum Ecol Risk Assess 25(1-2):81–103. https://doi.org/10.1080/10807039.2018.1480353

Panaskar DB, Wagh VM, Pawar RS (2017) Geochemical characterisation of fluoride containing groundwater from Sita Nadi Watershed, Bhokar Taluka, Maharashtra, India. J Earth Environ Sci (JEES), 145(10). https://doi.org/10.29011/JEES-145.10004

Pandith M, Kaplay RD, Potdar SS, Sangnor H, Rao AD (2017) Impact of urbanization coupled with drought situations on groundwater quality in shallow (basalt) and deeper (granite) aquifers with special reference to fluoride in Nanded-Waghala Municipal Corporation, Nanded District, Maharashtra (India). Environ Monit Assess 189(9):428

Panneerselvam B, Paramasivam SK, Karuppannan S, Ravichandran N, Selvaraj P (2020) A GIS-based evaluation of hydrochemical characterisation of groundwater in hard rock region, South Tamil Nadu, India. Arab J Geosci 13(17):1–22

Pawar NJ, Shaikh IJ (1995) Nitrate pollution of ground waters from shallow basaltic aquifers, Deccan Trap Hydrologic Province, India. Environ Geol 25:197–204. https://doi.org/10.1007/BF00768549

Pawar NJ, Pawar JB, Kumar S, Supekar A (2008) Geochemical eccentricity of ground water allied to weathering of basalts from the deccan volcanic province, India: Insinuation on CO2 consumption. Aquat Geochem 14(1):41–71. https://doi.org/10.1007/s10498-007-9025-9

Piper AM (1944) A graphic procedure in the geochemical interpretation of water analyses. Trans Am Geophys Union 25:914–928

Rao NS, Chaudhary M (2019) Hydrogeochemical processes regulating the spatial distribution of groundwater contamination, using pollution index of groundwater (PIG) and hierarchical cluster analysis (HCA): a case study. Groundw Sustain Dev 9:100238

Sawyer CN, McCarty PL (1967) Chemistry for sanitary engineers. McGraw-Hill, New York

Sethy SN, Syed TH, Kumar A, Sinha D (2016) Hydrogeochemical characterization and quality assessment of groundwater in parts of Southern Gangetic plain. Environ Earth Sci 75:232. https://doi.org/10.1007/s12665-015-5049-4

Sonkamble S, Sahya A, Mondal NC, Harikumar P (2012) Appraisal and evolution of hydrochemical processes from proximity basalt and granite areas of Deccan Volcanic Province (DVP) in India. J Hydrol 438–439:181–193. https://doi.org/10.1016/j.jhydrol.2012.03.022

Srinivas Y, Aghil TB, Hudson Oliver D, Nithya Nair C, Chandrasekar N (2017) Hydrochemical characteristics and quality assessment of groundwater along the Manavalakurichi coast, Tamil Nadu, India. Appl Water Sci 7:1429–1438. https://doi.org/10.1007/s13201-015-0325-8

Subba Rao N (2012) PIG: a numerical index for dissemination of groundwater contamination zones. Hydrol Process 26(22):3344–3350

Subba Rao N, Deepali M, Dinakar A et al (2017) Geochemical characteristics and controlling factors of chemical composition of groundwater in a part of Guntur district, Andhra Pradesh, India. Environ Earth Sci 76:747

Subba Rao N, Srihari C, Deepthi Spandana B, Sravanthi M, Kamalesh T, Jayadeep A (2019) Comprehensive understanding of groundwater quality and hydrogeochemistry for the sustainable development of sub-urban area of Visakhapatnam, Andhra Pradesh, India. Hum Ecol Risk Assess 25:52–80. https://doi.org/10.1080/10807039.2019.1571403

Subba Rao N, Ravindra B, Wu J (2020) Geochemical and health risk evaluation of fluoride rich groundwater in Sattenapalle Region, Guntur district, Andhra Pradesh, India. Hum Ecol Risk Assess 26(9):2316–2348. https://doi.org/10.1080/10807039.2020.1741338

Subramani T, Rajmohan N, Elango L (2010) Groundwater geochemistry and identification of hydrogeochemical processes in a hard rock region, Southern India. Environ Monit Assess 162(1):123–137

Thomas J, Joseph S, Thrivikramji KP (2015) Applied Geochemistry Hydrochemical variations of a tropical mountain river system in a rain shadow region of the southern Western Ghats, Kerala, India. Appl Geochem 63:456–471. https://doi.org/10.1016/j.apgeochem.2015.03.018

Tian Y, Zheng Y, Wu B, Wu X, Liu J, Zheng C (2015) Modeling surface water-groundwater interaction in arid and semi-arid regions with intensive agriculture. Environ Model Softw 63:170–184. https://doi.org/10.1016/j.envsoft.2014.10.011

USEPA (1980) Exposure and risk assessment for zinc. US Environmental Protection Agency Office of Water Regulations and Standards (WH-553). EPA440481016. PB85212009

USEPA (1989) Risk assessment guidance for superfund, Volume 1: Human health evaluation manual (Part A) (EPA/540/1-89/002: Interim Final). Office of Emergency and Remedial Response, Washington DC

USEPA (2008) Boron. RegulDeterm Support Doc SelContam from Second Drink Water Contam Candidate List (CCL 2) EPA Rep 815-R-08-012

USEPA (2014) Human health evaluation of manual, supplemental guidance: update of standard default exposure factors, OSWER Directive 9200.1-120. United State Environmental protection Agency, Washington (DC)

Vetrimurugan E, Elango L, Rajmohan N (2013) Sources of contaminants and groundwater quality in the coastal part of a river delta. Int J Environ Sci Technol 10:473–486. https://doi.org/10.1007/s13762-012-0138-3

Vincy MV, Brilliant R, Pradeepkumar AP (2015) Hydrochemical characterization and quality assessment of groundwater for drinking and irrigation purposes: a case study of Meenachil River Basin, Western Ghats, Kerala, India. Environ Monit Assess 187:4217. https://doi.org/10.1007/s10661-014-4217-4

Wagh VM, Panaskar DB, Varade AM, Mukate SV, Gaikwad SK, Pawar RS, Muley AA, Aamalawar ML (2016a) Major ion chemistry and quality assessment of the groundwater resources of Nanded tehsil, a part of southeast Deccan Volcanic Province, Maharashtra, India. Environ Earth Sci 75(21):1418

Wagh VM, Panaskar DB, Muley AA, Mukate SV, Lolage YP, Aamalawar ML (2016b) Prediction of groundwater suitability for irrigation using artificial neural network model: a case study of Nanded tehsil, Maharashtra, India. Model Earth Syst Environ 2(4):196

Wagh VM, Panaskar DB, Muley AA, Mukate SV (2017) Groundwater suitability evaluation by CCME WQI model for Kadava River Basin, Nashik, Maharashtra, India. Model Earth Syst Environ 3(2):557–565

Wagh VM, Panaskar DB, Mukate SV, Gaikwad SK, Muley AA, Varade AM (2018) Health risk assessment of heavy metal contamination in groundwater of Kadava River Basin, Nashik, India. Modeling Earth Systems and Environment 4(3):969–980

Wagh VM, Mukate SV, Panaskar DB, Muley AA, Sahu UL (2019a) Study of groundwater hydrochemistry and drinking suitability through water quality index (WQI) modelling in Kadava river basin, India. SN Appl Sci 1(10):1251

Wagh VM, Panaskar DB, Jacobs JA, Mukate SV, Muley AA, Kadam AK (2019b) Influence of hydro-geochemical processes on groundwater quality through geostatistical techniques in Kadava River basin, Western India. Arab J Geosci 12(1):7

Wagh VM, Panaskar DB, Mukate SV, Aamalawar ML, Laxman Sahu U (2020a) Nitrate associated health risks from groundwater of Kadava river basin Nashik, Maharashtra, India. Hum Ecol Risk Assess Int J 26(3):654–672

Wagh V, Mukate S, Muley A, Kadam A, Panaskar D, Varade A (2020b) Study of groundwater contamination and drinking suitability in basaltic terrain of Maharashtra, India through PIG and multivariate statistical techniques. J Water Supply Res Technol AQUA 69(4): 398–414

WHO (World Health Organization) (2017) Guidelines for drinking water quality, Library Cataloguing-in-Publication Data, NLM classification: WA 675, 4th edn. World Health Organization, Geneva

WHO (World Health Organization) (2009) Boron in drinking-water: background document for development of WHO guidelines for drinking-water quality (No. WHO/HSE/ WSH/09.01/2)

Zango MS, Sunkari ED, Abu M, Lermi A (2019) Hydrogeochemical controls and human health risk assessment of groundwater fluoride and boron in the semi-arid North East region of Ghana. J Geochem Explor 207:106363

Zhang Y, Wu J, Xu B (2018) Human health risk assessment of groundwater nitrogen pollution in Jinghui canal irrigation area of the loess region, northwest China. Environ Earth Sci 77:273